Carbohydrate Polymers 84 (2011) 713–726

Contents lists available at ScienceDirect

Carbohydrate Polymers

journal homepage: www.elsevier.com/locate/carbpol

MS^n of the six isomers of $(GlcN)_2(GlcNAc)_2$ aminoglucan tetrasaccharides (diacetylchitotetraoses): Rules of fragmentation for the sodiated molecules and application to sequence analysis of hetero-chitooligosaccharides

Balakumar Vijayakrishnan[a], Arisara Issaree[a], Yuri E. Corilo[b], Christina Ramires Ferreira[b], Marcos N. Eberlin[b], Martin G. Peter[a,b,*]

[a] Universität Potsdam, Institut für Chemie, Karl-Liebknecht-Str. 24-25, D-14476 Potsdam, Germany
[b] ThoMSon Mass Spectrometry Laboratory, Institute of Chemistry, University of Campinas - UNICAMP, Campinas, SP 13083-970, Brazil

ARTICLE INFO

Article history:
Received 9 October 2009
Received in revised form 25 March 2010
Accepted 22 April 2010
Available online 29 April 2010

Keywords:
Chitosan
Fragmentation
Oligosaccharides
Sequence analysis
Tandem mass spectrometry

ABSTRACT

The six possible isomers of di-*N*-acetylchitotetraoses [**AADD**, **ADDA**, **ADAD**, **DADA**, **DAAD**, and **DDAA**, where **D** stands for 2-amino-2-deoxy-β-D-glucose (GlcN) and **A** for 2-acetamido-2-deoxy-β-D-glucose (GlcNAc)] were analyzed by ESI(+)-MS^n. Collision induced dissociation via MS^n experiments were performed for the sodiated molecules of *m*/*z* 769 $[M+Na]^+$ for each isomer, and fragments were generated mainly by glycosidic bond and cross-ring cleavages. Rules of fragmentation were then established. A reducing end **D** residue yields the $^{0,2}A_4$ cross-ring $[M-59+Na]^+$ fragment of *m*/*z* 710 as the most abundant, whereas isomers containing a reducing end **A** prefer to lose water to form the $[M-18+Na]^+$ ion of *m*/*z* 751, as well as abundant $^{0,2}A_4$ cross-ring $[M-101+Na]^+$ fragments of *m*/*z* 668 and B_3 $[M-221+Na]^+$ ions of *m*/*z* 548. MS^3 of C- and Y-type ions shows analogous fragmentation behaviour that allows identification of the reducing end next-neighbour residue. Due to gas-phase anchimeric assistance, B-type cleavage between the glycosidic oxygen and the anomeric carbon atom is favoured when the glycon is an **A** residue. Relative ion abundances are generally in the order B ≫ C > Y, but may vary depending on the next neighbour towards the non-reducing end. These fragmentation rules were used for partial sequence analysis of hetero-chitooligosaccharides of the composition $\mathbf{D_2A_3}$, $\mathbf{D_3A_3}$, $\mathbf{D_2A_4}$, $\mathbf{D_4A_3}$, and $\mathbf{D_3A_4}$.

1. Introduction

Oligosaccharides of β-1,4 linked D-glucosamine (abbreviated here as **D**) and/or *N*-acetyl-D-glucosamine (**A**), also named chitooligosaccharides (CHOs), belong to the sub-class of aminoglucans (Peter, 2002a, 2002b). They are structurally related to lipochitooligosaccharides (LCO's), which contain basically a backbone of *N*-acyl-$\mathbf{D}(\mathbf{A})_n$ ($n = 3$–6) where the **D** residue is nearly always located at the non-reducing end and *N*-acylated with a long-chain fatty acid (for a review, see Spaink, 2000). Similar to LCO's, which induce nodulation in legumes (Mathesius, 2003; Price, 1999; Spaink, 2000), CHOs are biological signaling molecules with a variety of remarkable activities, being involved in pattern formation during embryonic development in vertebrates (Bakkers et al., 1997; Semino & Allende, 2000) and elicitation of phytoalexins in plants (dos Santos, El Gueddari, Trombotto, & Moerschbacher, 2008; Vander, Vårum, Domard, El Gueddari, & Moerschbacher, 1998). Other biological effects of CHOs, such as immunostimulant, anticancer, antimicrobial and antioxidant activities, have been described (Kim & Rajapakse, 2005) and some CHOs are under development for pharmaceutical applications (Einarsson, Gislason, Peter, & Bahrke, 2003). Within a research program on protein–ligand interactions of chitinolytic enzymes and chitolectins (Bahrke, 2007; Cederkvist et al., 2006; Germer, Muegge, Peter, Rottmann, & Kleinpeter, 2003; Houston et al., 2002; Vaaje-Kolstad, Houston, et al., 2004; Vaaje-Kolstad, Vasella, et al., 2004; van Aalten et al., 2001), we are interested in rapid and sensitive methods for structure determination of CHOs. NMR spectroscopy requires relatively large amounts of sample and yields limited information because of an insufficient resolution for higher CHOs (Vårum, Anthonsen, Grasdalen, & Smidsrød, 1991a, 1991b), thus leaving mass spectrometry (MS) as the method of choice (Peter & Eberlin, in press).

CHOs composed exclusively of either **D** or **A** are named homo-CHOs, whereas those containing both monosaccharide units are termed hetero-CHOs. Analysis of homo-CHOs by MS is rather straightforward. As there are no isomers (except conformers and reducing end anomeric stereoisomers), their structures are easily

* Corresponding author at: Universität Potsdam, Institut für Chemie, Karl-Liebknecht-Str. 24-25, D-14476 Potsdam, Germany. Tel.: +49 331 9775424; fax: +49 331 6014757.
E-mail address: Martin.Peter@uni-potsdam.de (M.G. Peter).

0144-8617/$ – see front matter © 2010 Elsevier Ltd. All rights reserved.
doi:10.1016/j.carbpol.2010.04.041

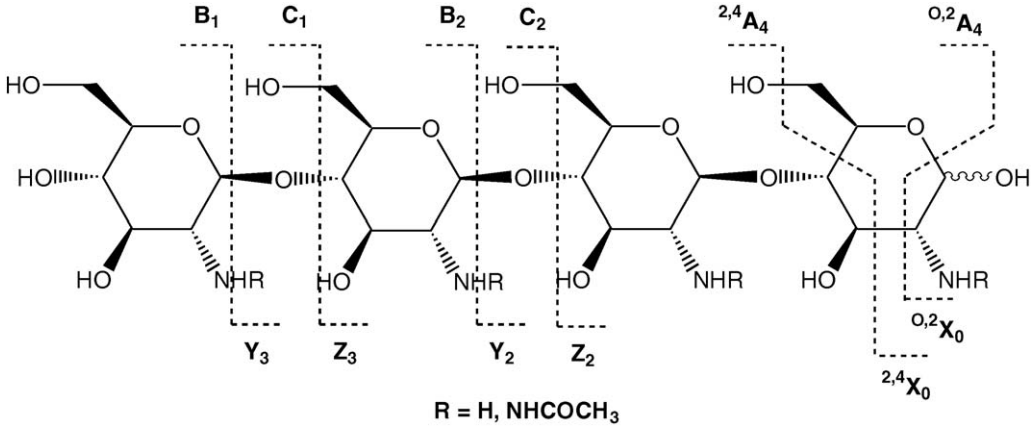

Fig. 1. Nomenclature for the assignment of fragment ions of AGO tetrasaccharides according to Domon and Costello (1988).

deduced from their molecular mass which are a multiple of the number of **D** or **A** residues plus water, i.e. ($\mathbf{D}_n + H_2O$) or ($\mathbf{A}_n + H_2O$), respectively.

The molecular mass of a hetero-CHO reveals, however, only its DP and F_A, but is silent about structure, since any hetero CHO of the composition $\mathbf{D}_n\mathbf{A}_m$ can exist as a number of constitutional isomers only differing in the position of the **D** and **A** residues in the oligosaccharide chain. Characterization of hetero-CHOs is therefore a formidable structural challenge, in particular when a sample is available only as an intractable mixture of isomers. For such mixtures, the task must be handled by fragmentation of molecules with sequential MS (MS^n). MS^n has been shown to be a powerful technique for structural elucidation, well established and widely applied in glycobiology (Budnik, Lee, & Steen, 2006; Fernandez, 2007; Wolff, Amster, Chi, & Linhardt, 2007). Product ions generated by MS^n of oligosaccharides are assigned according to the nomenclature proposed by Domon and Costello (1988), as Fig. 1 illustrates for CHO tetrasaccharides.

Cross-ring and glycosidic bond fragmentation of protonated molecules have been observed in FAB(+)-MS and FAB(−)-MS of $\mathbf{D}_n$ (n = 3–9) and $\mathbf{A}_m$ (m = 3–6) (Bosso & Domard, 1992) and in (+)-FAB-MS^2 of $\mathbf{A}_m$ (m = 1–6) (Singh, Gallagher, Derrick, & Crout, 1995). MALDI(+)-TOF MS of sodiated $\mathbf{D}_n$ (n = 2–12) molecules show weak $^{0,2}A_n$ fragments of each oligomer (Trombotto, Ladaviere, Delolme, & Domard, 2008). In ESI(+)-MS, B- and C-type ions of protonated molecules of CHOs are the most abundant whereas sodiated molecules dissociate also by ^{0,2}A- and ^{2,4}A-type cleavages, as shown by CID, SORI CID, EID, and ECD MS^2 of $\mathbf{D}_7$ and $\mathbf{A}_5$ (Budnik, Haselmann, Elkin, Gorbach, & Zubarev, 2003). MS^n studies of CHOs have been summarized in a recent review (Peter & Eberlin, in press).

MS^n sequence analysis of hetero-CHOs is described in only few publications. Reductive amination with an aromatic amine, such as 2-aminoacridone or 3-(acetylamino)-6-aminoacridine, introduces a tag at the reducing-end. Tagged, sodiated Y-type fragments predominate, as has been shown in sequence analysis of complex mixtures of hetero-CHOs by MALDI-TOF PSD MS (Bahrke et al., 2002), linear ion trap MALDI MS^2 and MS^3 (Haebel, Bahrke, & Peter, 2007), and by MALDI-TOF MS^2 (Cederkvist, Parmer, Varum, Eijsink, & Sørlie, 2008). Due to the fatty acid residue located at the non-reducing end sugar residue, a tag is inherently present in LCO's, Nevertheless, structure elucidation of LCO's by MS can be rather tricky, due to various additional substituents, including glycosylation of the CHO backbone (for an excellent, timeless review, see Van der Drift, Olsthoorn, Brull, Blok-Tip, & Thomas-Oates, 1998).

Chemical derivatization cannot be used to identify a CHO that is non-covalently bound to a protein and in equilibrium with a mixture of CHOs. Sequence analysis must then rely on gas phase MS fragmentation of the native (underivatized) hetero-CHOs. This task has been achieved so far in only one case by *top-down* nano-ESI-MS^2 of protonated molecules of $\mathbf{D}_2\mathbf{A}_3$ bound to a chitinase (Cederkvist et al., 2006).

The aim of the work reported herein was to establish general rules for the CID chemistry of underivatized hetero-CHOs during ESI(+)-MS^n. Sodiated molecules of the six constitutional isomers of $\mathbf{D}_2\mathbf{A}_2$ (Fig. 2) were therefore investigated systematically by ESI(+)-MS^2. The fragmentation rules were then applied to partial sequence analysis of five hetero-CHOs of unknown isomer composition.

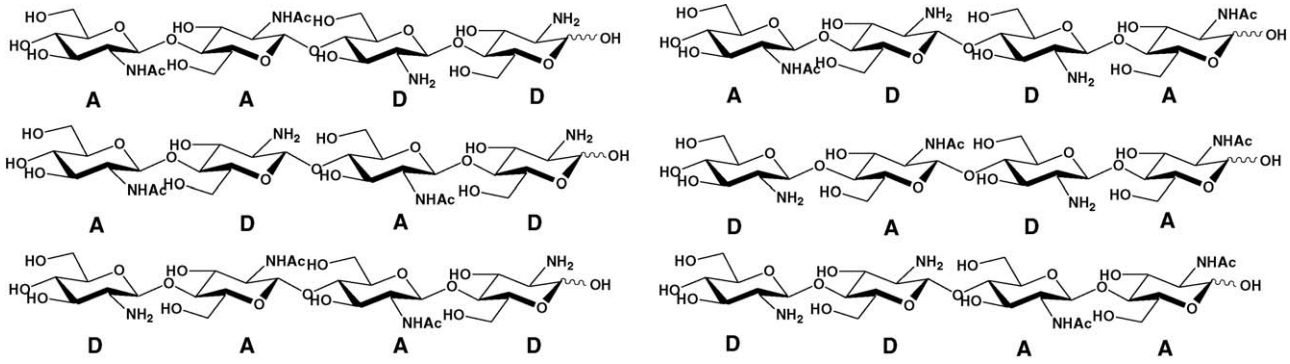

Fig. 2. Structures of the six constitutional isomers of $\mathbf{D}_2\mathbf{A}_2$.

2. Materials and methods

2.1. Samples

The AGO tetramers **AADD**, **ADDA**, **ADAD**, **DADA**, **DAAD**, and **DDAA** were synthesized as described elsewhere (Issaree, 2008; Vijayakrishnan, 2008). Solvents and chemicals used for sample preparation were of highest purity, as available from local suppliers.

2.2. Mass spectrometry

Samples of synthetic CHO tetramers and hetero-chitooligosaccharides were dissolved in methanol/water (1:1 or 1:2) to give concentrations of ca. 0.1 mg mL^{-1}. Solutions were spiked with ca. 0.1% NaCl for favoured monitoring of sodiated molecules and loaded into 96-well plates (total volume of 100 μL in each well). The LTQ FTMS ultra, a hybrid mass spectrometer (Thermo Scientific, Waltham, MA, USA) equipped with a Triversa NanoMate 100 (Advion BioSciences, Ithaca, NY, USA) for chip-based nano-ESI MS (Zhang, Van Pelt, & Henion, 2003) was used for the experiments. Only the linear quadrupole ion trap mass analyzer was used for the experiments, since there was no need of high accuracy m/z measurements. General conditions were: pressure of 20 mbar and an electrospray voltage of ca. 1.5 kV. All MS^n experiments were performed and analyzed in the linear ion trap mass analyser by varying the collision-induced dissociation (CID) after the m/z of the interest had been isolated. Helium was used as the collision gas, collision energies (CE) were between 10 and 30 eV. Spectra were processed with the Xcalibur Qual Browser software, Version 2.0.2.0 (Thermo Electron Corporation, U.S.A., 1998–2006).

3. Results and discussion

3.1. General considerations

Cross-ring $^{0,2}A_4$ and $^{2,4}A_4$ fragments are expected as $[M-59+Na]^+$ and $[M-119+Na]^+$ for a reducing end **D** and as $[M-101+Na]^+$ and $[M-161+Na]^+$ for a reducing end **A** residue, respectively. Cleavage of glycosidic bonds of the six isomeric tetrasaccharides gives series of two trisaccharide fragments of the $\mathbf{DA}_2$ or $\mathbf{D}_2\mathbf{A}$ compositions, three disaccharide, i.e. $\mathbf{D}_2$, (**DA**), or $\mathbf{A}_2$, and two monosaccharide fragments, i.e. **D** or **A**, respectively. The C_3- and Y_3-type ions are of the same $\mathbf{D}_2\mathbf{A}$ isobaric composition for **ADDA** and $\mathbf{DA}_2$ for **DAAD**, but they differ for the other four isomers, i.e. C_3 of **AADD** and **ADAD** has the composition $\mathbf{DA}_2$, whereas **DDAA** and **DADA** give $\mathbf{D}_2\mathbf{A}$. The corresponding Y-type ions will appear as matching peaks with an increment of ±42 Da.

Assignments of peaks can be ambiguous because several possibilities generating isobaric ions (Table 1):

(1) elimination of acetamide and ^{0,2}A-type cross-ring fragmentation of a reducing end **D** residue (−59 Da)
(2) Y-type loss of a non-reducing end neutral **D** residue and $^{2,4}A_4$ cross-ring fragments of a reducing end **A** residue (−161 Da),
(3) B- and Z-type ions of the same composition $\mathbf{D}_n\mathbf{A}_m$-H_2O,
(4) C- and Y-type ions of the same composition $\mathbf{D}_n\mathbf{A}_m$,

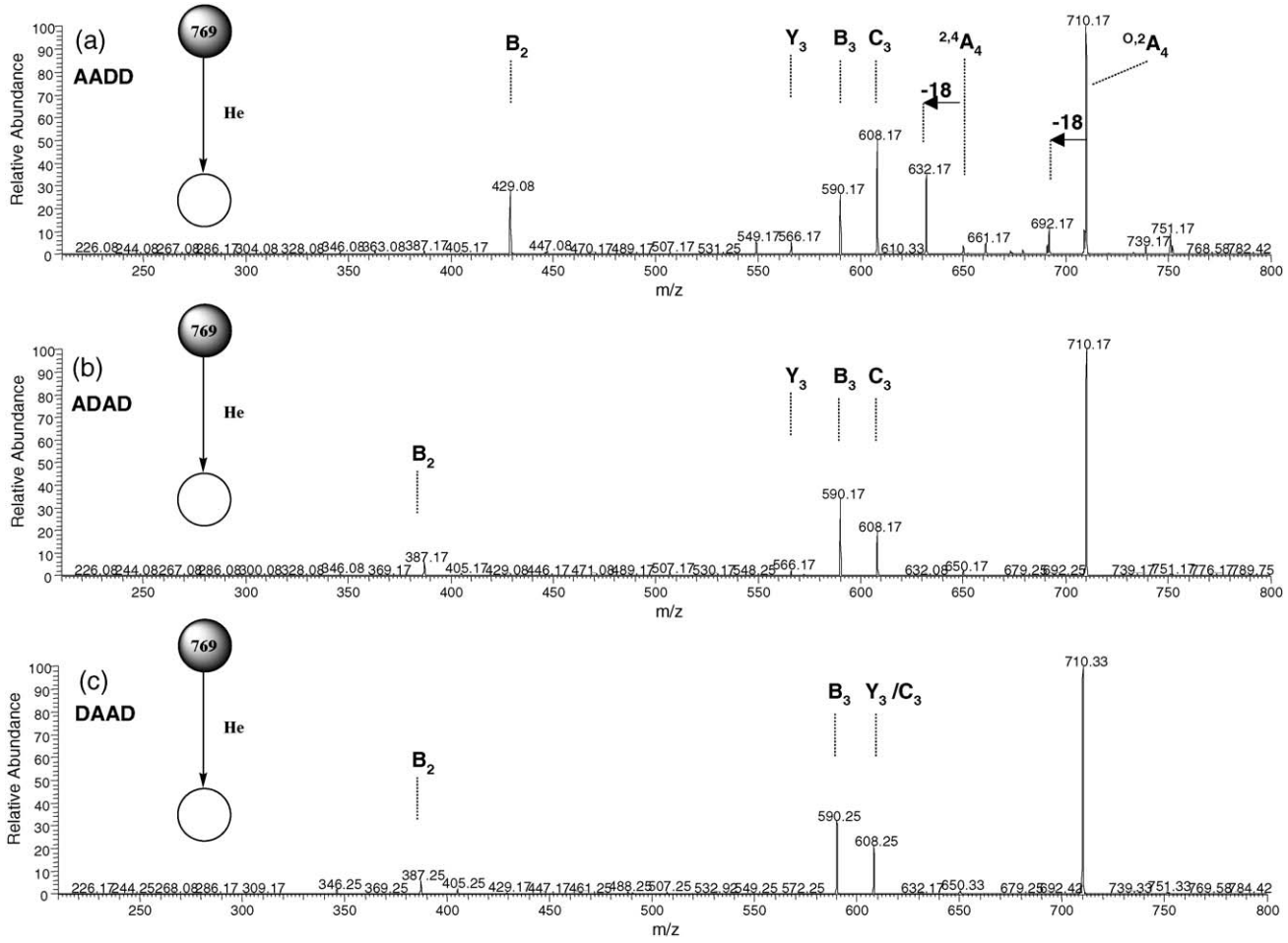

Fig. 3. MS^2 of the ion of m/z 769 $[M+Na]^+$ for (a) **AADD** (CE 14), (b) **ADAD** (CE 30) and (c) **DAAD** (CE 15).

Table 1
Mass reductions (in Da) calculated for fragmentation processes.

Fragmentation	$^{0,2}A_4$	$^{2,4}X_4$	$^{0,2}X_4$	B_1	Y_1	C_1	Z_1	$^{2,4}A_4$
D	−59	−60	−120	−161	−179	−179	−161	−119
A	−101	−60	−120	−203	−221	−221	−203	−161

Elimination	NH_3	H_2O	H_2CO	H_2C_2O	CH_3CONH_2
	−17	−18	−30	−42	−59

(5) the $^{2,4}X_0$ fragment of a reducing end **A** residue is isobaric with the B_1 ion of a non-reducing end **D** residue (*m*/*z* 184),
(6) loss of ketene (−42 Da) may suggest a "false" **D** residue.

3.2. MS^2 of sodiated molecules of m/z 769 $[M+Na]^+$

MS^2 of the $[M+Na]^+$ ion of *m*/*z* 769 of the tetrasaccharides **AADD**, **ADAD**, and **DAAD** show the base $[M-59+Na]^+$ ion of *m*/*z* 710 that accounts for $^{0,2}A_4$ cross-ring fragmentation of the reducing end **D** (Fig. 3). $^{2,4}A_4$ cross-ring fragments are observed as trace $[M-119+Na]^+$ ions of *m*/*z* 650 (Fig. 3). Ions of *m*/*z* 608, accounting for loss of a **D** are C_3 ions of the composition $\mathbf{DA_2}$ from **AADD** and **ADAD** (Fig. 3a, b), and isobaric C_3 and Y_3 ions from **DAAD** (Fig. 3c). Y_3 ions of *m*/*z* 566 and $\mathbf{D_2A}$ composition are detected with low abundance in the MS^2 of **AADD** and **ADAD**. B_3 fragment ions of *m*/*z* 590 and B_2 ions of *m*/*z* 429 and 387, respectively, are also detected. The Z_3 ion of both **AADD** and **ADAD** expected to have the same *m*/*z* 548 value, is virtually absent, indicating that Z-type fragmentation is insignificant.

MS^2 of tetramers **ADDA**, **DADA**, and **DDAA** show loss of water as leading to the main $[M-18+Na]^+$ fragment of *m*/*z* 751 (Fig. 4). $^{0,2}A_4$ cross-ring $[M-101+Na]^+$ fragments of *m*/*z* 668 are of low abundance for **ADDA** and **DADA** (Fig. 4a, b) but quite significant for **DDAA** (Fig. 4c). The minor $[M-161+Na]^+$ ions of *m*/*z* 608 are isobaric $^{2,4}A_4$ cross-ring fragments of the reducing end **A**, and/or Y type ions formed by loss of a non-reducing end **D** residue of **DADA** and **DDAA**, respectively. The MS^2 data also show low abundant ions of *m*/*z* 590, barely detectable for **DDAA**, corresponding to $[^{2,4}A_4-18+Na]^+$ for all three isomers, but also for $[Z_3+Na]^+$ for **DADA** and **DDAA**, respectively. Otherwise, B_3 ions of *m*/*z* 548 of the $\mathbf{D_2A}$ composition are very abundant, appearing even as the base ion for **DDAA**. The ions of *m*/*z* 405 are assigned to the isobaric C_2 and Y_2 ions of **ADDA** and **DADA**, where the B_2 ion of *m*/*z* 387 is also detected. MS^2 of **DDAA** gives the Y_2 ion of *m*/*z* 447 and the B_2 ion of *m*/*z* 345.

X-type ions formed by cross-ring fragmentation of the reducing end sugar are expected to be detected in the low *m*/*z* range ($m/z \leq 184$) with low abundance, if at all, and are not considered. Loss of acetamide is insignificant, since the $[M-59+Na]^+$ ion of *m*/*z*

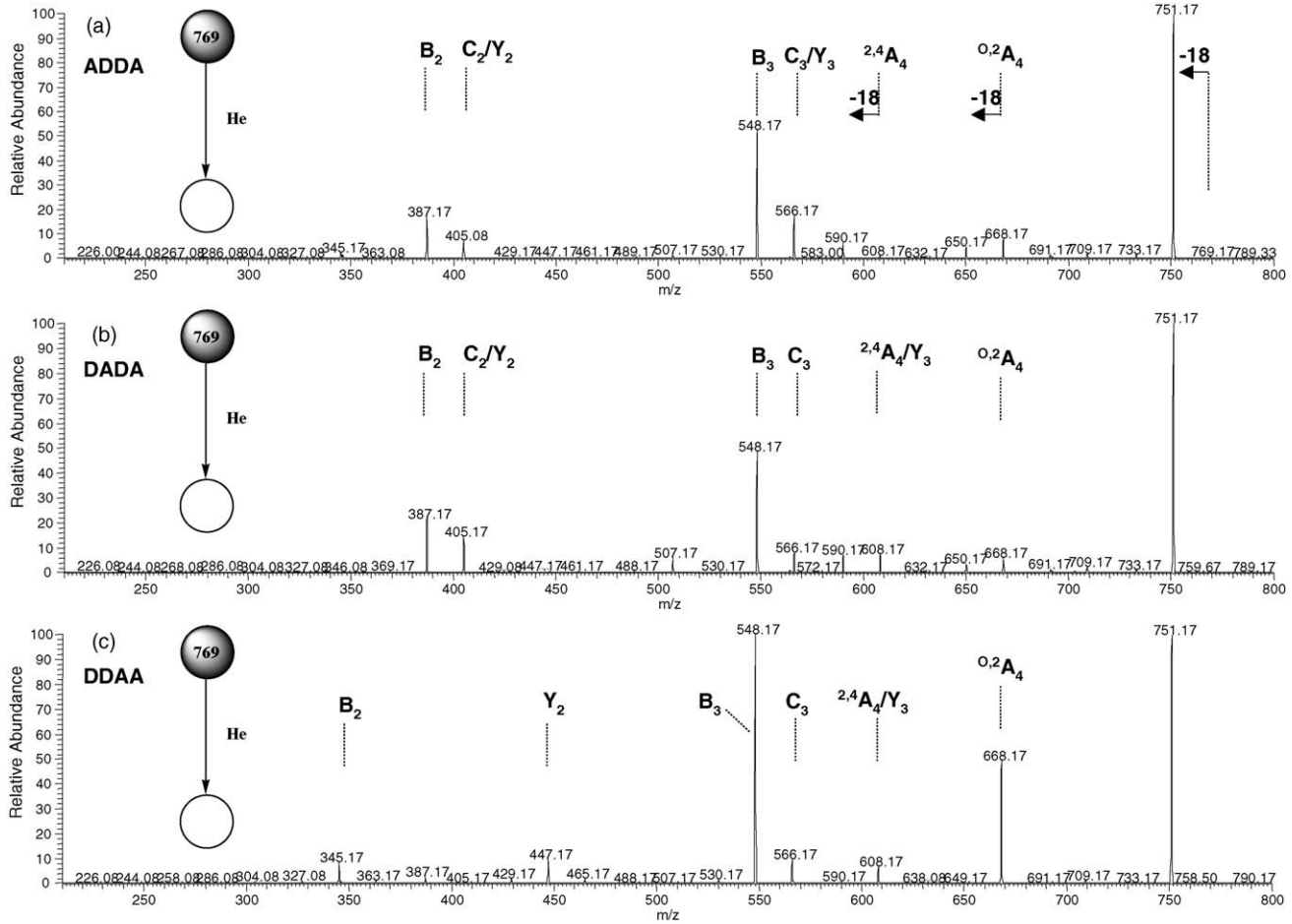

Fig. 4. MS^2 of the ion of *m*/*z* 769 $[M+Na]^+$ for (a) **ADDA** (CE 13), (b) **DADA** (CE 15), and (c) **DDAA** (CE 15).

710 is absent in MS^2 of **ADDA**, **DADA**, and **DDAA**. For **AADD**, the trace $[M-161, -59+Na]^+$ ion of *m/z* 549 indicates the $^{0,2}A_3$ cross-ring fragment, rather than loss a **D** and of acetamide. The *m/z* 549 ion is virtually absent in MS^2 of **ADAD**, and **DAAD**.

Multiphoton dissociation (IR-MPD) and electron-capture dissociation (ECD) of the sodiated molecules of **ADDA**, **DAAD**, and **DDAA** reveal analogous patterns of cross-ring and glycosidic bond cleavages, with more abundant fragment ions in the lower *m/z* range (Fig. S1). The diagnostic value of the ions of *m/z* < 280 is questionable, however, due to isobaric fragment ions which cannot be identified by MS^n (Fig. S2).

3.3. MS^n of cross-ring fragments of m/z 710 $[^{0,2}A_4+Na]^+$ of reducing end **D** tetrasaccharides

The MS^3 scan *m/z* 769 → *m/z* 710 $[^{0,2}A_4+Na]^+$ → products for **AADD** shows a major fragment of *m/z* 632 $[^{0,2}A_4-78+Na]^+$ due to loss of water and two molecules of formaldehyde (Fig. 5a). The B_3 and B_2 ions of *m/z* 590 and 429, respectively, are also detected. The MS^4 scan *m/z* 769 → *m/z* 710 → *m/z* 632 → products gives mainly the B_2 ion as well as a weak C_2 ion of *m/z* 447, the corresponding $^{0,2}A_2$ cross-ring fragment of *m/z* 346 and the B_1 ion of *m/z* 226 (Fig. 5b). Fig. S3 summarizes the fragmentation pattern of sodiated **AADD**.

The MS^3 scan *m/z* 769 → *m/z* 710 $[^{0,2}A_4+Na]^+$ → products for **ADAD** and **DAAD** reveals a different fragmentation pattern. The most abundant fragment is that of *m/z* 590 $[B_3+Na]^+$ (Fig. 5c, d). Other abundant fragment ions account for the loss of 60 Da (*m/z* 650), equivalent to two molecules of formaldehyde, and for the $[B_2+Na]^+$ ion of *m/z* 387. Thus, it appears that MS^3 of $^{0,2}A_4$ ions of sodiated **AADD**, **ADAD**, and **DAAD** yields preferentially the B_3 ion when the next glycon neighbour is **A**, but loss of water and formaldehyde is favoured when the next neighbour is **D**.

The observation of abundant B_3 ions of the composition $\mathbf{DA}_2$ in the MS^3 of *m/z* 710 of sodiated **AADD**, **ADAD**, and **DAAD** as well as the very low abundance or even absence of ions of *m/z* 549 supports the conclusion that loss of a 59 Da species from $[M+Na]^+$ of *m/z* 769 is caused by $^{0,2}A_4$ cross-ring fragmentation rather than by elimination of acetamide from an intrachain **A** residue (*vide supra*).

3.4. MS^n of cross-ring fragments of m/z 668 $[^{0,2}A_4+Na]^+$ of reducing end **A** tetrasaccharides

The $^{0,2}A_4$ fragments of sodiated **ADDA**, **DADA**, and **DDAA** are observed in the MS^2 of the ion of *m/z* 769 $[M+Na]^+$ as well as the ions of *m/z* 668 $[M-101+Na]^+$ (see Fig. 4). The MS^3 scan *m/z* 769 → *m/z* 668 $[^{0,2}A_4+Na]^+$ → products shows loss of water (−18 Da) and two molecules of formaldehyde (−60 Da), that is $[^{0,2}A_4-78+Na]^+$, and this process prevails when the next neighbour of the fragmented reducing end **A** residue is **D**, whereas the B_3 ion is preferred when the next neighbour is **A** (Fig. 6). This fragmentation behaviour is analogous to that of the $^{0,2}A_4$ fragments of reducing end **D** tetrasaccharides (cf. MS^3 of the ion of *m/z* 710, Fig. 5).

The MS^4 scan *m/z* 769 → *m/z* 668 → *m/z* 590 → products for sodiated **DADA**, which is equivalent with $[^{2,4}A_4-18+Na]^+$, shows a major ion of *m/z* 387 $[B_2+Na]^+$ (Fig. 6d). The minor ions of *m/z*

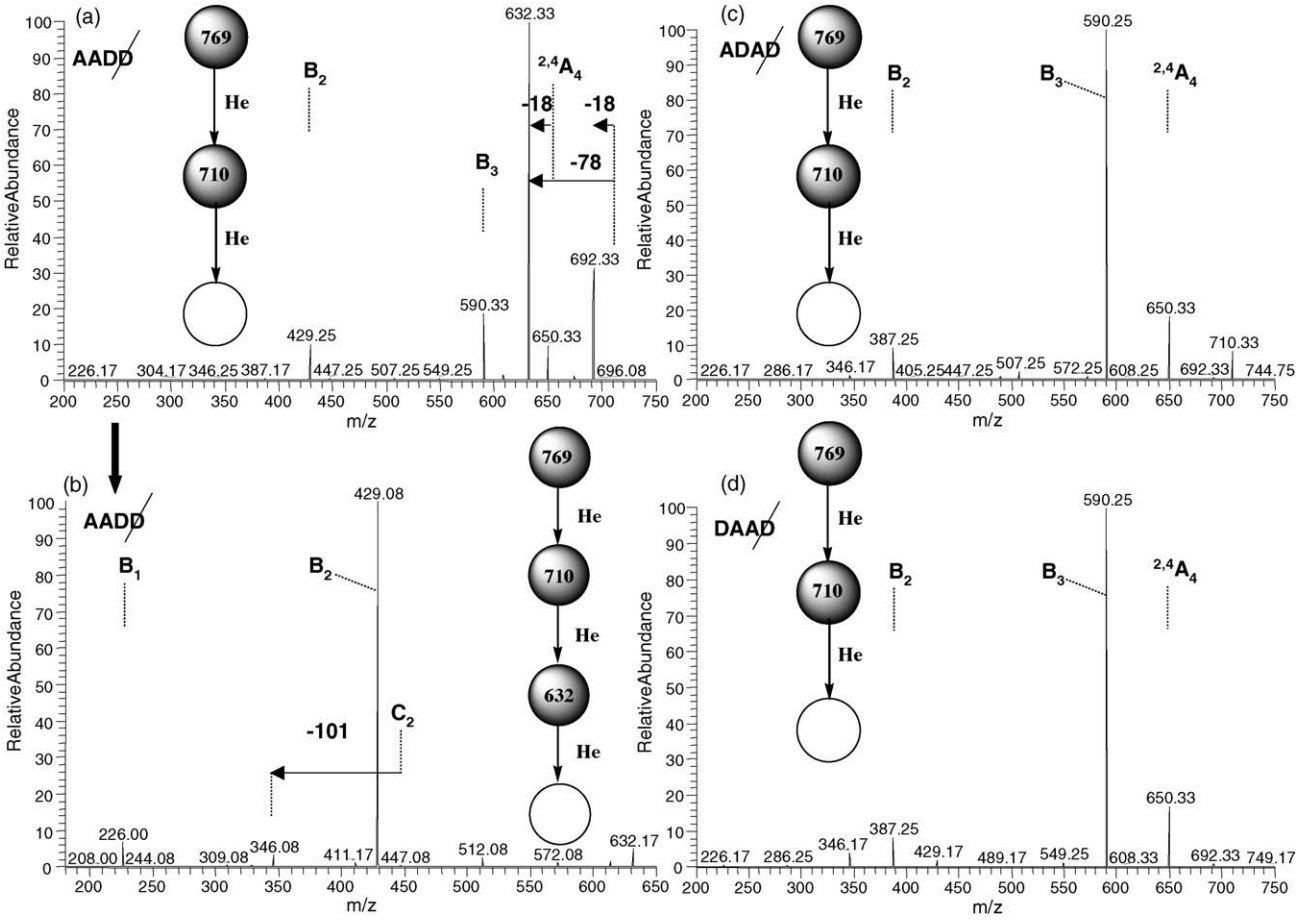

Fig. 5. (a) MS^3 scan *m/z* 769 $[M+Na]^+$ → *m/z* 710 $[^{0,2}A_4+Na]^+$ → products for **AADD**. (CE_{MS2} 14; CE_{MS3} 30), (b) MS^4 scan *m/z* 769 $[M+Na]^+$ → *m/z* 710 $[^{0,2}A_4+Na]^+$ → *m/z* 632 $[^{0,2}A_4-78+Na]^+$ → products for **AADD** (CE_{MS2} 14; CE_{MS3} 14; CE_{MS4} 10), (c) MS^3 scan *m/z* 769 $[M+Na]^+$ → *m/z* 710 $[^{0,2}A_4+Na]^+$ → products for **ADAD** (CE_{MS2} 15; CE_{MS3} 11.5), and (d) **DAAD** (CE_{MS2} 15; CE_{MS3} 15).

429, 286, and 226 are assigned to $[^{2,4}A_3-18+Na]^+$, $[^{0,2}A_2-18+Na]^+$ and $[^{2,4}A_2-18+Na]^+$, respectively. Fig. S4 explains the correlation of fragment ions observed by the MS^4 scan of m/z 769 → m/z 668 → m/z 590 → products for sodiated **DADA**.

3.5. MS^n of the ion of m/z 608 $[^{2,4}A_4+Na]^+$ of reducing end **A**, and/or $[C_3+Na]^+$ of reducing end **D**, and/or $[Y_3+Na]^+$ of non-reducing end **D** tetrasaccharides

As discussed above (see Figs. 3 and 4), MS^2 yield trisaccharide fragments of m/z 608 $[M-161+Na]^+$ which account for $\mathbf{A_2D}$, that is C_3 ions of **AADD** and **ADAD** and Y_3 ions of **DADA** and **DDAA**, whereas they are isobaric C_3 and Y_3 ions of **DAA** and **AAD** from **DAAD**, respectively. MS^3 of the ion of m/z 608 must therefore yield cross-ring fragments that account for either a **D** or an **A** residue at the reducing end of these trisaccharide ions. In addition, $^{2,4}A_4$ cross-ring fragments of reducing end **A** tetramers must be considered.

Fig. 7 shows MS^3 data of the ion of m/z 608 of **AADD**, **ADAD**, and **DAAD**. The reducing end **D** residue of the C_3 ion of **AADD** is confirmed by the major ion of m/z 549 $[C_3-59+Na]^+$, accounting for the $^{0,2}A_3$ cross-ring fragment (Fig. 7a). The corresponding $^{2,4}A_3$ ion of m/z 489 appears with low abundance. C_2 and B_2 ions as well as a low abundant Y_2 ion of m/z 447, 429, and 405, respectively, are also detected. The $^{0,2}A_2$ fragment ion of m/z 346 confirms the presence of the **A** residue at the non-reducing end which also gives a weak B_1 ion of m/z 226.

The C_3 ion of m/z 608 of **ADAD** contains an **A** residue at the reducing end. Loss of water gives the very abundant ion B_3 of m/z 590 (Fig. 7b). Low abundant ions of cross-ring cleavages are also observed: m/z 507 for $^{0,2}A_3$ and m/z 346 for $^{0,2}A_2$. As the minor ion of m/z 489 $[C_3-119+Na]^+$ cannot be a cross-ring fragment of a **D** residue, and it must be formed by $^{0,2}A_3$ cross-ring fragmentation and water loss of the reducing end **A** residue of **ADA**. Similarly, since a C_2/Y_2 ion of the composition $\mathbf{A_2}$ is not possible, those of m/z 447 and 429 must represent $^{2,4}A_3$ cross-ring fragments from the reducing end **A** residue plus loss of water, respectively. The major ion of m/z 387 is attributed to $[B_2+Na]^+$. The C_2/Y_2, C_1/Y_1, and B_1 fragment ions of m/z 405, 244, and 226, respectively, are also detected.

As confirmed by MS^3 (Fig. 7c), the **DAAD** fragment ion of m/z 608 is composed of the isobaric C_3 and Y_3 ions of the composition $\mathbf{DA_2}$, The relative abundance of the ion of m/z 549 [$^{0,2}A_3$ of $Y_3+Na]^+$ is lower than that of m/z 507 [$^{0,2}A_3$ of $C_3+Na]^+$. Considering that the major ion in the MS^2 of an oligosaccharide bearing a **D** residue at the reducing end results from $^{0,2}A_3$ cross-ring cleavage, but from water loss from a reducing end **A** residue, it is concluded that the **DAA** C_3 ion is the major and the **AAD** Y_3 ion is the minor component of the ion population of m/z 608 of sodiated **DAAD**. The ions of m/z 447 and 429 are consistent with the C_2/Y_2 ions of $\mathbf{A_2}$ composition and the corresponding B_2 ion, respectively. The major ion of m/z 387 is the B_2 fragment of the C_3 ion. Assignment of the remaining fragment ions in the MS^3 of the ion of m/z 608 of **DAAD** is straightforward in analogy with MS^3 of **AADD** and **ADAD**.

Minor fragment ions of m/z 608 are also observed in the MS^2 of **ADDA**, **DADA**, and **DDAA** (see Fig. 4), accounting for $^{2,4}A_4$ cross-ring fragments of the reducing end **A** residue of all three tetramers, but also for Y_3 ions of **DADA** and **DDAA** (Fig. 8). As **ADDA** does not contain a reducing or a non-reducing end **D** residue, the loss of a

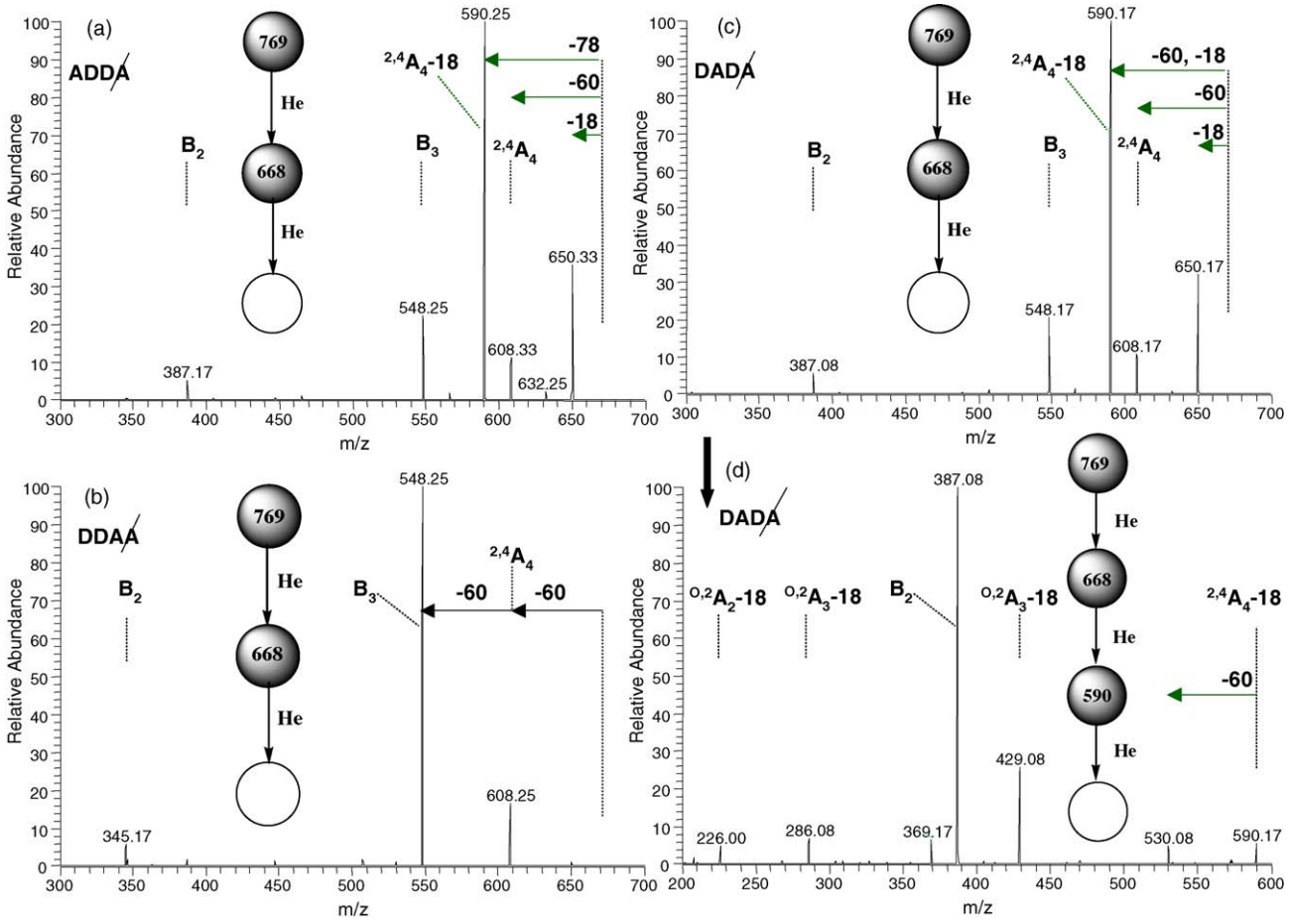

Fig. 6. MS^3 scan m/z 769 $[M+Na]^+$ → m/z 668 $[^{0,2}A_4+Na]^+$ → products for (a) **ADDA** (CE_{MS2} 20; CE_{MS3} 12), (b) **DDAA** (CE_{MS2} 15; CE_{MS3} 15), (c) **DADA** (CE_{MS2} 15; CE_{MS3} 12). (d) MS4 scan m/z of 769 $[M+Na]^+$ → m/z 668 $[^{0,2}A_4+Na]^+$ → m/z 590 $[^{0,2}A_4-78+Na]^+$ → products for **DADA** (CE_{MS2} 15; CE_{MS3} 12; CE_{MS4} 12).

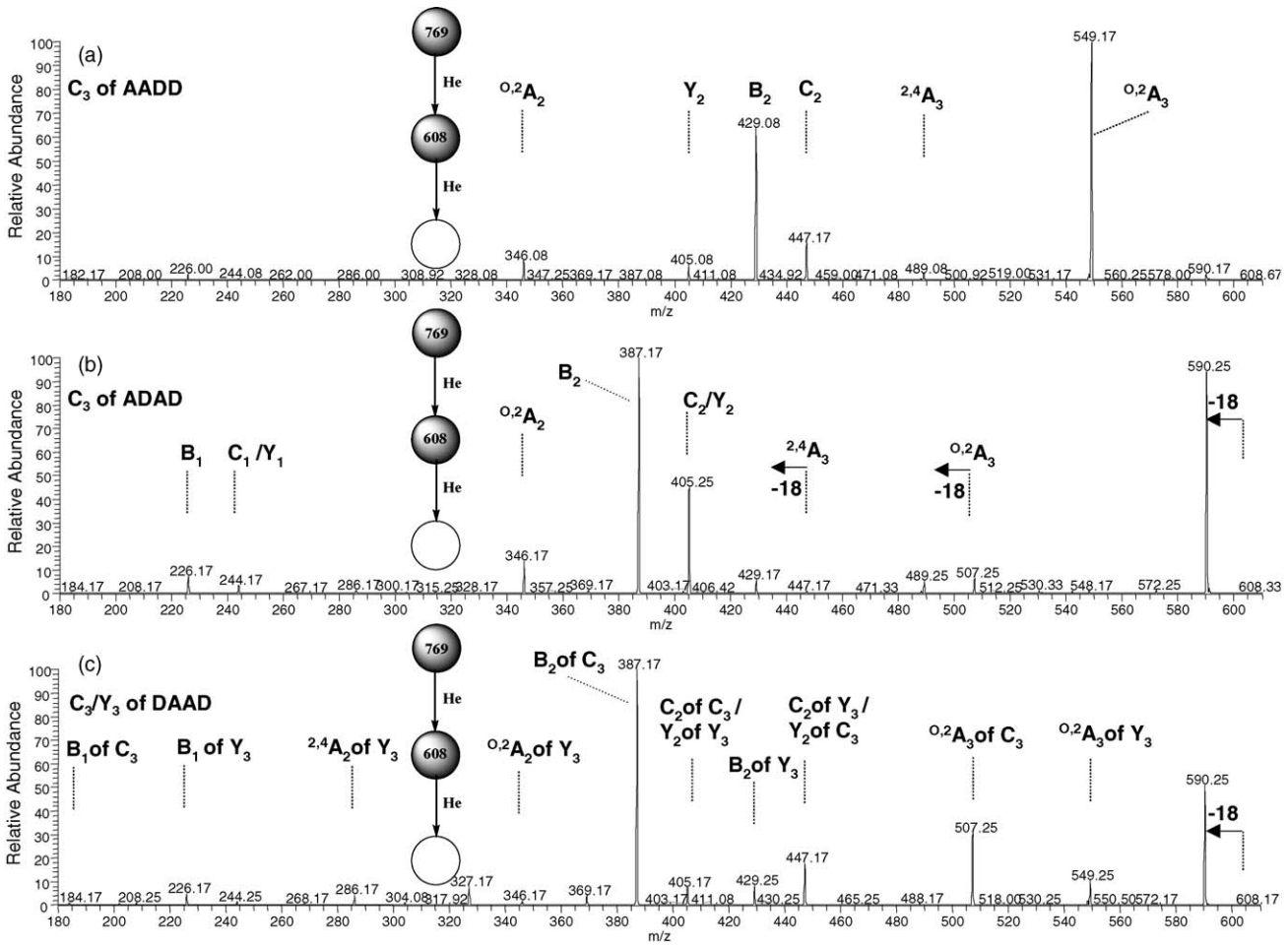

Fig. 7. MS^3 scan m/z 769 $[M+Na]^+ \rightarrow m/z$ 608 $[C_3+Na]^+ \rightarrow$ products for and/or $[Y_3+Na]^+$, respectively, for (a) **AADD** (CE_{MS2} 14; CE_{MS3} 14), (b) **ADAD** (CE_{MS2} 15; CE_{MS3} 12), (c) **DAAD** (CE_{MS2} 15; CE_{MS3} 14).

neutral of 161 Da in MS^2 of **ADDA** (see Fig. 4) can only be due to $^{2,4}A_4$ cross-ring fragmentation which is confirmed by MS^3 of m/z 608, showing the base $[^{2,4}A_4-18+Na]^+$ ion of m/z 590 and the B_3 ion of m/z 548 (Fig. 9a). The C_2 ion (**AD**) of m/z 405 and the B_2 (**AD**) ion of m/z 387 are also detected. The trace ion of m/z 346 (Fig. 9a, inset) is due to $^{0,2}A_2$ cross-ring cleavage, whereas the ion of m/z 345, accounting for a $\mathbf{D}_2$ unit, is ambiguous. C_1 and B_1 ions of m/z 244 and 226 are observed with low abundances.

MS^3 of the ion of m/z 608 of **DADA** and **DDAA** detects the $^{2,4}A_4$ and Y_3 ions (Fig. 9b, c). The B_3 ion of m/z 548 is of lower abundance for **DADA** than **DDAA**, indicating a preference for B-type cleavage of the glycosidic bond of an **A** residue as compared with a **D** residue. Also, the $^{0,2}A_3$ cross-ring fragment of m/z 507 of the Y_3 ion is less abundant in the MS^3 of the ion of m/z 608 of **DADA** than that of **DDAA**.

3.6. MS^n of the ion of m/z 566 $[C_3+Na]^+$ of reducing end **A** and/or $[Y_3+Na]^+$ of non-reducing end **A** tetrasaccharides

Fragments of $\mathbf{D_2A}$ composition, i.e. $[M-203+Na]^+$ ions of m/z 566 (see Figs. 3 and 4), are observed in the MS^2 of five of the six isomers accounting for C_3 ions of **DADA** and **DDAA**, Y_3 ions of **AADD** and **ADAD**, and the isobaric C_3 and Y_3 ions of **ADDA**, respectively.

MS^3 of m/z 566 of **ADDA** confirms the presence of isobaric C_3 and Y_3 ions which are clearly distinguished by abundant ions of m/z 507 [$^{0,2}A_3$ of **ADD**$+Na]^+$ and the rather weak ion of m/z 465 [$^{0,2}A_3$ of **DDA**$+Na]^+$, as well as the B_2 ions of m/z 387 [B_2 of **ADD**$+Na]^+$ and m/z 345 [B_2 of **DDA**$+Na]^+$, respectively (Fig. 10a). The MS^3 of the ion of m/z 566 of **DADA** and **DDAA** are complimentary, showing the expected fragmentation of the C_3 ion with the **DAD** and **DDA** structures, with also the expected series of $^{0,2}A_3$, C_2 and B_2 ions, respectively (Fig. 10b, c).

Assignment of ions in the MS^3 of the ion of m/z 566 $[Y_3+Na]^+$ of **AADD** and **ADAD** is rather straightforward (Fig. 11). $^{0,2}A_3$ cross-ring cleavage of the reducing end **D** residue yields the major ion of m/z 507 in the MS^3 of both tetramers. The Y_3 ion **ADD** of **AADD** shows also the $^{0,2}A_2$ cross-ring fragment of m/z 346 with relatively high abundance. The minor ions of m/z 447 $[Y_3-119+Na]^+$ account for $^{2,4}A_3$ fragment ions. The remaining ions are assigned to the B_2 and C_2 ions. Other fragments appear as trace ions only and are of questionable significance.

3.7. Rules of fragmentation

Based on the analysis of the various types of cross-ring and glycosidic bond fragmentations, the following rules could be established:

Cross-ring cleavage:

1. A reducing end **D** residue gives mainly the $^{0,2}A_n$ fragment ion $[M-59+Na]^+$ whereas $^{2,4}A_n$ fragments $[M-119+Na]^+$ are minor (Fig. 3).
2. A reducing end **A** residue preferentially gives $[M-18+Na]^+$. $^{0,2}A_n$-type ions appear with lower abundances. The assignment of $^{2,4}A_n$ is ambiguous when there is a **D** residue located at the non-reducing end (Fig. 4).

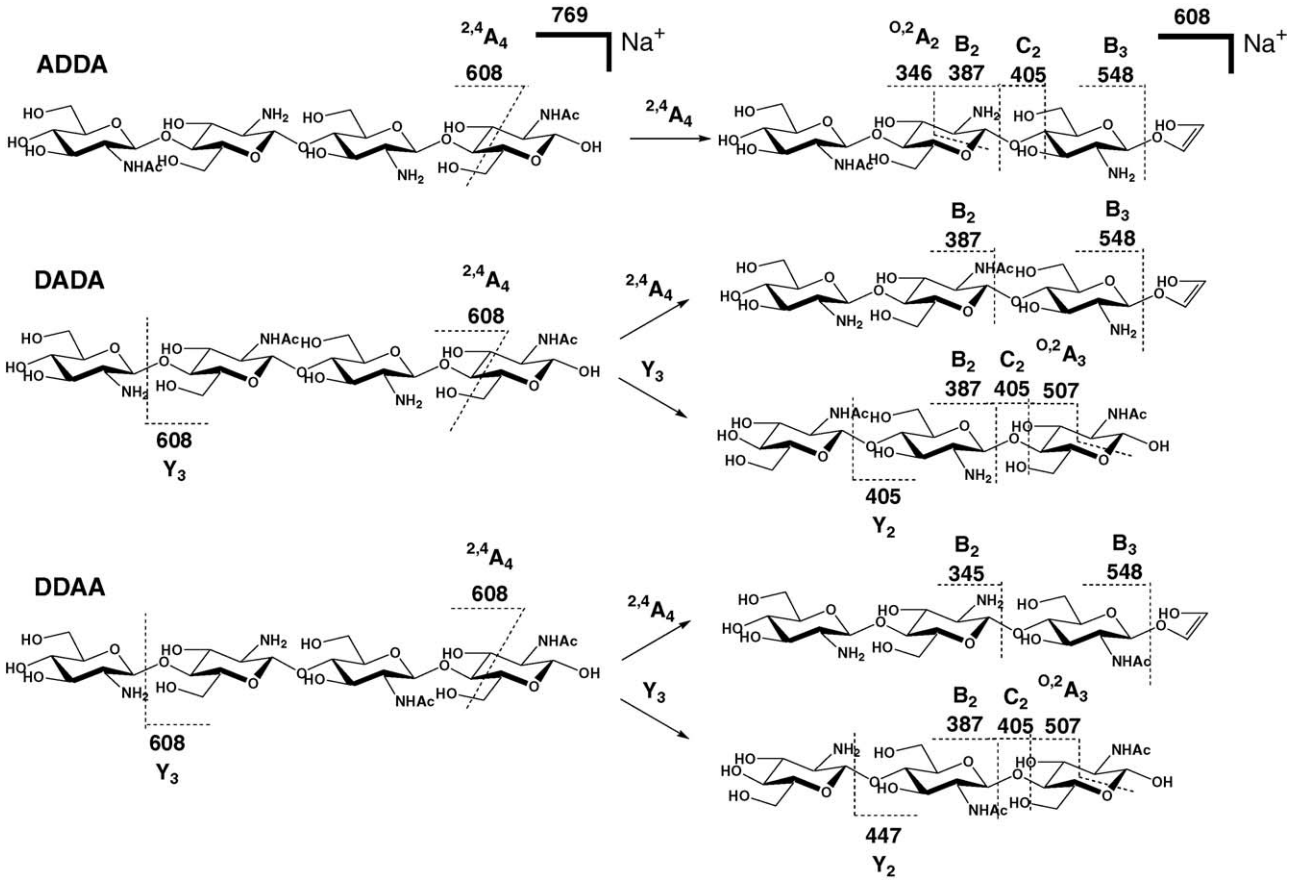

Fig. 8. MS^3 fragments expected for m/z 769 $[M+Na]^+ \rightarrow m/z$ 608→ products for **ADDA**, **DADA**, and **DDAA**.

3. $^{O,2}A_n$ fragment ions of a reducing end **A** residue are relatively more abundant when the next neighbour is **A** as compared to **D** (Fig. 4).
4. MS^3 of $^{O,2}A_n$ and $^{2,4}A_n$ fragment ions yields an abundant B_{n-1} ion when the next neighbour is **A**, but further fragmentation by loss of water and formaldehyde occurs when the next neighbour is **D** (Figs. 5 and 9).
5. X-type ions are minor, if detected at all. They are not diagnostic for distinguishing reducing end and non-reducing end **D** and **A** residues due to ambiguities in the assignment of isobaric fragment ions.

Glycosidic bond fragmentation:

6. The ion abundances for cleavage decrease generally in the order B > C > Y, with the exception of –**D**–O–**D**–, where C > B > Y (cf. Budnik et al., 2003).
7. In MS^2, B-type fragmentation of glycosidic bonds are favoured for –**A**–O–**A**– and –**A**–O–**D**–, but disfavoured for–**D**–O–**D**– and –**D**–O–**A**.
8. Z-type fragment ions are detected at trace abundances, if at all.

Table 2 and rules 7 and 8 summarize the relative abundances of the C, Y, and B type ions observed by MS^n of the six tetrasaccharides (Figs. 3, 4, 8 and 10).

Other two general observations:

9. Elimination of acetamide is insignificant.
10. An assignment of the trace fragment ions of $m/z \leq 286$ to a non-reducing end **D** or **A** residue is ambiguous because of the occurrence of isobars arising from loss of ketene (Fig. S2).

Table 2
Relative abundances of fragment ions from CID glycosidic bond cleavages in ESI(+)-MS^n of ($\mathbf{D_2A_2}$) isomers.

Trisaccharide fragments		Disaccharide fragments	
AADD	**ADDA**	**AADD**	**ADDA**
$C_3 > B_3 \gg Y_3$	$B_3 > C_3/Y_3$	$B_2 \gg C_2 > Y_2$	$B_2 > C_2/Y_2$
ADAD	**DADA**	**ADAD**	**DADA**
$B_3 > C_3 \gg Y_3$	$B_3 > C_3 > Y_3$	$B_2 > C_2/Y_2$	$B_2 > C_2/Y_2$
DAAD	**DDAA**	**DAAD**	**DDAA**
$B_3 > C_3/Y_3$	$B_3 \gg C_3 > Y_3$	$B_2 > C_2/Y_2$	$B_2 \approx C_2 \gg Y_2$

It is known that strongly coordinating metal ions direct fragmentations of oligosaccharides. As has been described for $\mathbf{A_2}$ and $\mathbf{A_3}$ (Cancilla, Wong, Voss, & Lebrilla, 1999), cross-ring cleavages are charge-remote but glycosidic bond cleavages are charge-induced. The preferential cross-ring cleavages are therefore reasonably explained with a stronger coordination of the alkali metal ion to **D** bearing a free amino group, as compared with **A** bearing an acetamido group. But glycosidic bond cleavage at an **A** unit is facilitated by anchimeric assistance of the acetamido group, and this assistance is unfeasible for B-type cleavage of the glycosidic bond of a **D** residue (Fig. 12).

MS^n experiments were performed also with ions of m/z 650 $[^{2,4}A_4+Na]^+$ of reducing end **D** and $[^{O,2}A_4-18+Na]^+$ of reducing end **A** tetrasaccharides, as well as with ions of m/z 590 and 548 $[B_3+Na]^+$. The data are in agreement with the fragmentation rules, as discussed in the supplement.

3.8. Analysis of mixtures of unknown isomer composition

According to the fragmentation rules, it should be possible to gain at least partial sequence information of isomers $\mathbf{D}_n\mathbf{A}_m$ by MS^n of ^{O,2}A-, C/Y-, and B-type ions. We have therefore investigated

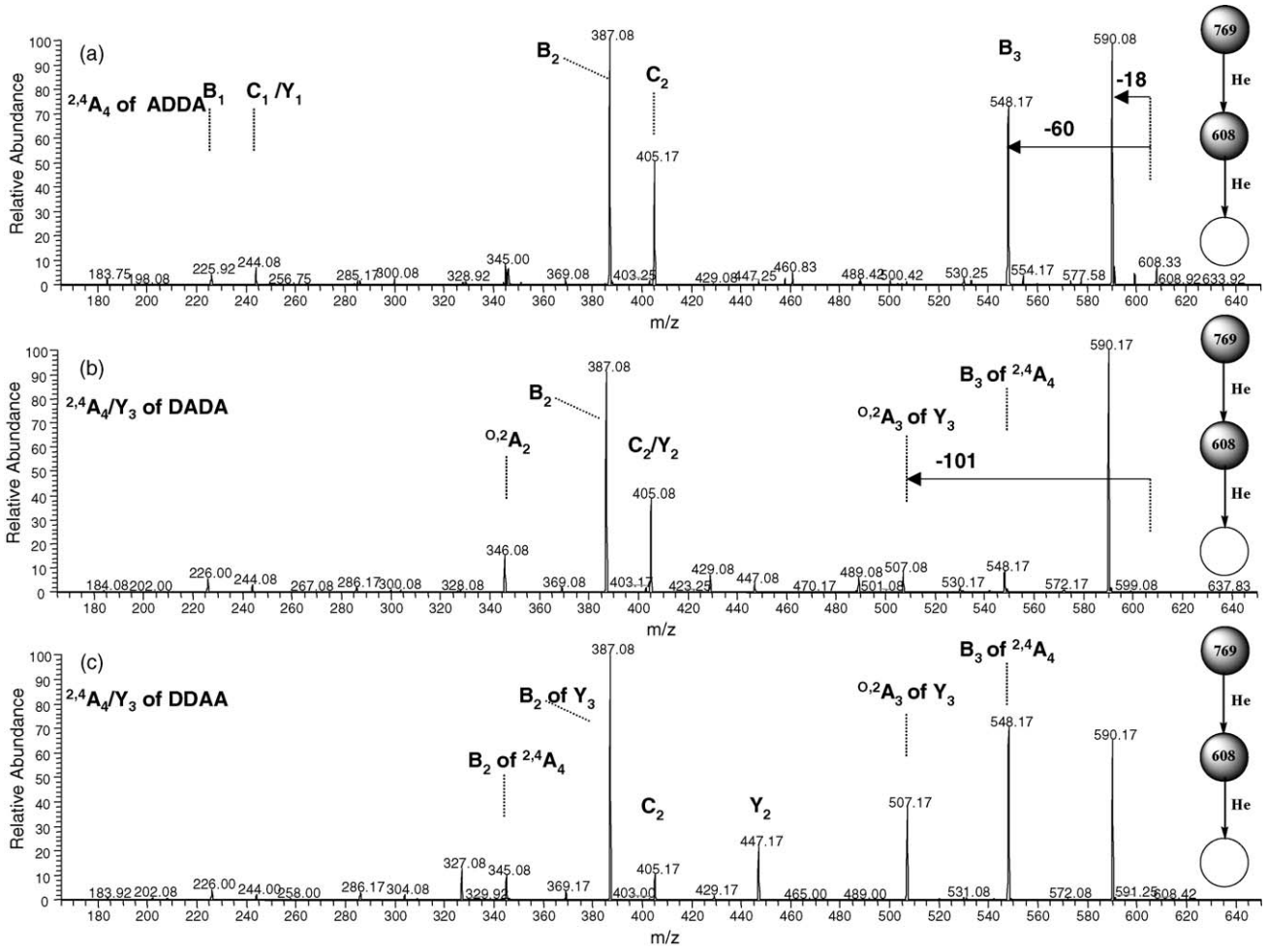

Fig. 9. MS^3 scan m/z 769 $[M+Na]^+ \rightarrow m/z$ 608 $[^{2,4}A_4+Na]^+ \rightarrow$ products and/or $[Y_3+Na]^+$, respectively, for (a) **ADDA** (CE_{MS2} 20; CE_{MS3} 11), (b) **DADA** (CE_{MS2} 20; CE_{MS3} 16), (c) **DDAA** (CE_{MS2} 15; CE_{MS3} 12).

CHOs obtained by size exclusion chromatography of an enzymatic hydrolyzate of chitosan (cf. Bahrke et al., 2002). ESI(+)-MS of the sample reveals a complex mixture of oligomers and homologs (Fig. 13), from which the sodiated molecules of the pentasaccharide $\mathbf{D_2A_3}$, two hexasaccharides, $\mathbf{D_3A_3}$ and $\mathbf{D_2A_4}$, and two heptasaccharides, $\mathbf{D_4A_3}$ and $\mathbf{D_3A_4}$,were selected for analysis.

3.9. MS^n of m/z 972 $[M+Na]^+$ ($\boldsymbol{D_2A_3}$)

Permutation of the positions of two **D** and three **A** residues of pentasaccharide $\mathbf{D_2A_3}$ gives ten isomers, i.e.

1. DAAAD	**2. ADAAD**	**3. AADAD**	**4. AAADD**	**5. DDAAA**
6. DADAA	**7. DAADA**	**8. ADDAA**	**9. ADADA**	**10. AADDA**

MS^2 of the $[M+Na]^+$ ion of m/z 972 (Fig. 14) shows the base $[M-18+Na]^+$ ion of m/z 954 and an $^{O,2}A_5$ fragment of m/z 871 $[M-101+Na]^+$. Reducing end **D** isomers **1**–**4** are excluded because of the absence of a $^{O,2}A_5$ fragment ion of m/z 913 $[M-59+Na]^+$ (rule 1). The $^{2,4}A_5$ fragments of m/z 811 $[M-161+Na]^+$ of reducing end **A** residues are isobaric with Y_4 ions of isomers **5**–**7**. According to rules 2 and 6, both $^{2,4}A_5$ and Y_4 fragment ions are expected to be formed with low intensity. The complete absence of ions of m/z 650 $[Y_3+Na]^+$ and 345 $[B_2+Na]^+$ in MS^2 (Fig. 14, inset), though eventually expected to result with low intensity from **5** (**DDAAA**), suggests that this **5** is absent and hence the ion of m/z 811 is generated by $^{2,4}A_5$ cross-ring rather than by Y_4 glycosidic bond fragmentation. The relatively strong B_4 ion of m/z 751 $[M-203+Na]^+$, together with the corresponding C_4 ion of m/z 769, is of the $\mathbf{D_2A_2}$ composition. Isobaric Z_4 and Y_4 ions could be formed from isomers **4**–**6**, respectively. According to rule 8, the Z_4 ion is insignificant, whereas Y_4 would give a minor contribution to the ion of m/z 769 (rule 6). The two B_3 ions of m/z 590 ($\mathbf{DA_2}$) and 548 ($\mathbf{D_2A}$) indicate that both **D** and **A** occur as next neighbours of the reducing end **A**. The MS^3 scan m/z 972 $[M+Na]^+ \rightarrow m/z$ 769 $[C_4+Na]^+ \rightarrow$ products shows diagnostic cross-ring fragments of m/z 710 $[^{O,2}A_4+Na$ of $(\mathbf{DA_2})$-$\mathbf{D}]^+$ and m/z 668 $[^{O,2}A_4+Na$ of $(\mathbf{D_2A})$-$\mathbf{A}]^+$ as well as two B_3 ions of m/z 590 and 548, and three B_2 ions of m/z 429, 387, and 345, respectively, accounting for the six reducing end **A** isomers **5**–**10** of $(\mathbf{D_2A_2})$-**A** (Fig. 15). Since isomer **5** is unlikely, the ion of m/z 345 is assigned to the B_2 ion of Y_4 of isomer **8**. In summary, pentasaccharide $\mathbf{D_2A_3}$ is a mixture of isomers **6**–**10** with those containing an **A** residue in the second position, i.e. **6** and **8**, as major components.

Other minor cross-ring fragments are ions of m/z 507 $[^{O,2}A_3+Na+$ of C_4 (**DA**)-**DA**] and 286 $[^{2,4}A_2$ of C_4 **AD**-(**DA**)]. The ions of m/z 912 $[M-60+Na]^+$ and 834 $[M-120-18+Na]^+$ are obviously generated by non-diagnostic X-type fragmentations of a non-reducing end **D** or **A** residue (cf. Table 1).

3.10. MS^n of m/z 1133 $[M+Na]^+$ ($\boldsymbol{D_3A_3}$)

The 20 possible isomers of $\mathbf{D_3A_3}$ are

1. DDAAAD	**2. DADAAD**	**3. DAADAD**	**4. DAAADD**	**5. ADDAAD**
6. ADADAD	**7. ADAADD**	**8. AADDAD**	**9. AADADD**	**10. AAADDD**
11. DDDAAA	**12. DDADAA**	**13. DDAADA**	**14. DADDAA**	**15. DADADA**
16. DAADDA	**17. ADADDA**	**18. AADDDA**	**19. ADDDAA**	**20. ADDADA**

Isomers **1**–**16** are excluded because the $^{0,2}A_6$ ion of m/z 1074 $[M-59+Na]^+$ and the $^{2,4}A_6/Y_5$ ion of m/z 972 $[M-161+Na]^+$ are

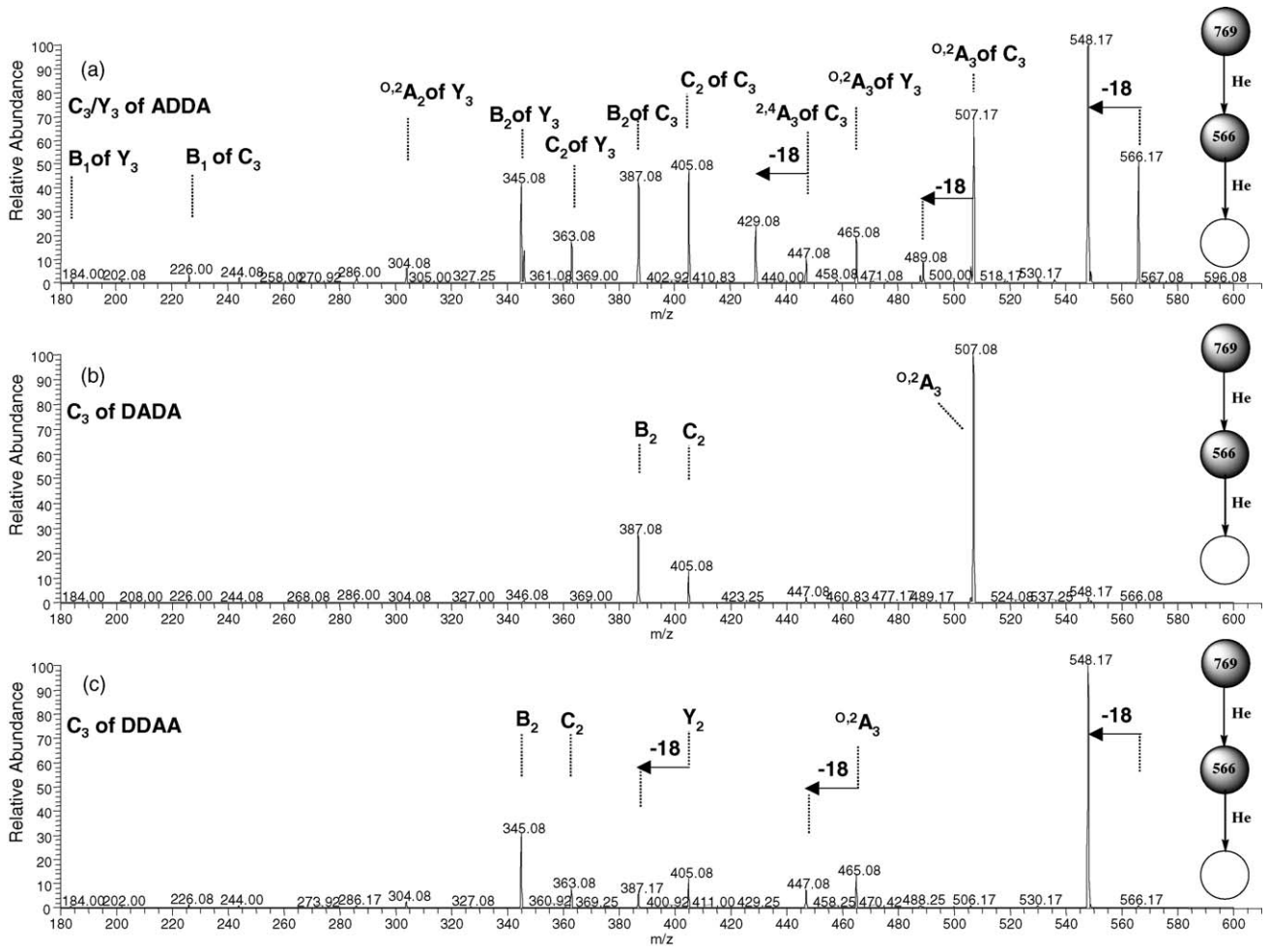

Fig. 10. MS^3 scan m/z 769 $[M+Na]^+ \rightarrow m/z$ 566 $[C3+Na]^+ \rightarrow$ products for (a) **ADDA** (CE_{MS2} 20; CE_{MS3} 10), (b) **DADA** (CE_{MS2} 20; CE_{MS3} 12), (c) **DDAA** (CE_{MS2} 15; CE_{MS3} 12).

absent in the MS^2 of the $[M+Na]^+$ ion of *m/z 1133* (Fig. S12). MS^3 scan $[M+Na]^+ \rightarrow m/z$ 930 $[C_5/Y_5+Na]^+ \rightarrow$ products gives, besides $^{0,2}A_5$ cross-ring fragments of reducing end **D** (minor) and **A** (major), two B_4 ions of m/z 751 ($\mathbf{D_2A_2}$) and 709 ($\mathbf{D_3A}$), consistent with isomers **17**–**20** (Fig. S13). The occurrence of only B_3 ion of m/z 548 ($\mathbf{D_2A}$) and one B_2 ion of m/z 387 (**DA**), and the absence of B- type fragments $\mathbf{DA_2}$ (calcd. m/z 590) and $\mathbf{A_2}$ (calcd. m/z 429) excludes isomers **17** and **18**. In summary, ($\mathbf{D_3A_3}$) is a mixture of isomers **19** (major) and **20** (minor).

3.11. MS^n ofthe $[M+Na]^+$ ion of m/z 1175 ($\mathbf{D_2A_4}$)

The 15 possible isomers of $\mathbf{D_2A_4}$ are

1. AAAADD	**2. AAADAD**	**3. AADAAD**	**4. ADAAAD**	**5. DAAAAD**
6. AAADDA	**7. AADADA**	**8. ADAADA**	**9. DAAADA**	**10. AADDAA**
11. ADDAAA	**12. ADADAA**	**13. DAADAA**	**14. DADAAA**	**15. DDAAAA**

Isomers **1**–**5** are excluded because an $^{0,2}A_6$ ion of m/z 1116 $[M-59+Na]^+$ is absent in MS^2 of the $[M+Na]^+$ion of m/z 1175 (Fig. S14). The reducing end **A** is confirmed by the $[M-18+Na]^+$ base ion of m/z 1157, by the $^{0,2}A_6$ cross-ring fragment of the $[M-101+Na]^+$ion of m/z 1074, and the corresponding, very weak isobaric $^{2,4}A_6/Y_5$ ions of $[M-161+Na]^+$ of m/z 1014. B_4 ions of m/z 793 (minor) and 751 (major) account, together with the corresponding C_4/Y_4 ions of m/z 769 and 811, for partial sequences of isomers **6**–**15**. Isomers having **D** in the second position, i.e. **6**–**9**, are excluded because an $^{0,2}A_5$ ion (calcd. m/z 913 $[C_5-59+Na]^+$) is absent in MS^3 scan m/z 1175 ($\mathbf{D_2A_4}$) $\rightarrow m/z$ 972 $[C_5/Y_5$ ($\mathbf{D_2A_3}$)$+Na]^+ \rightarrow$ products (Fig. S15). The base $[M-18+Na]^+$ ion of m/z 954 and the $^{0,2}A_5$ cross-ring fragment $[C_5-101+Na]^+$ ion of m/z 871 confirm the reducing-end **–A–A** sequence. Isomer **15** is excluded, as fragments of $\mathbf{A_3}$ (calcd. m/z 650 $[Y_3+Na]^+$) and $\mathbf{D_2}$ (calcd. m/z 363 $[C_2+Na]^+$) are absent. The strong B_4 ion of m/z 751 ($\mathbf{D_2A_2}$) and the corresponding C_4/Y_4 ion of m/z 769 account for partial sequences of isomers **10**–**14**. The homologous trace ions of m/z 811 and 793 are consistent with $[^{0,2}A_5+Na]^+$ and $[^{0,2}A_5-18+Na]^+$ of $[C_5+Na]^+$ of isomers **10**–**14**. The MS^4 scan m/z 1175 ($\mathbf{D_2A_4}$) $\rightarrow m/z$ 972 $\rightarrow m/z$ 769 $[C_4+Na]^+$ ($\mathbf{D_2A_2}$) $\rightarrow$ products shows unexpectedly abundant, non-diagnostic $^{0,2}X_3$ and $^{2,4}X_3$ fragment ions of m/z 709 $[C_4-60+Na]^+$ and 649 $[C_4-120+Na]^+$ (Fig. S16). The absence of cross-ring fragment ions of a reducing end **D** of m/z 710 $[^{0,2}A_4+Na]^+$ and 650 $[^{2,4}A_4+Na]^+$ excludes isomers **10**, **12**, and **13**. In summary, MS^2 excludes **1**–**5**, MS^3 excludes **6**–**9** and **15** and MS^4 excludes **10**, **12**, and **13**. The remaining two isomers are **11** (**ADDAAA**) and **14** (**DADAAA**).

3.12. MS^n of the $[M+Na]^+$ ion of m/z 1294 ($\mathbf{D_4A_3}$)

The 35 possible isomers of ($\mathbf{D_4A_3}$) are

1. AAADDDD	**2. AADADDD**	**3. AADDADD**	**4. AADDDAD**	**5. ADAADDD**
6. ADADADD	**7. ADADDAD**	**8. ADDAADD**	**9. ADDADAD**	**10. ADDDAAD**
11. DAAADDD	**12. DAADADD**	**13. DAADDAD**	**14. DADAADD**	**15. DADADAD**
16. DADDAAD	**17. DDAAADD**	**18. DDAADAD**	**19. DDADAAD**	**20. DDDAAAD**
21. AADDDDA	**22. ADADDDA**	**23. ADDADDA**	**24. ADDDADA**	**25. DAADDDA**
26. DADADDA	**27. DADDADA**	**28. DDAADDA**	**29. DDDAADA**	**30. DDADADA**
31. DADDDAA	**32. DDADDAA**	**33. ADDDDAA**	**34. DDDADAA**	**35. DDDDAAA**

MS^2 of the $[M+Na]^+$ ion of m/z 1294 excludes **1**–**20** by the absence an $^{0,2}A_4$ ion of m/z 1235 $[M-59+Na]^+$ of a reducing end

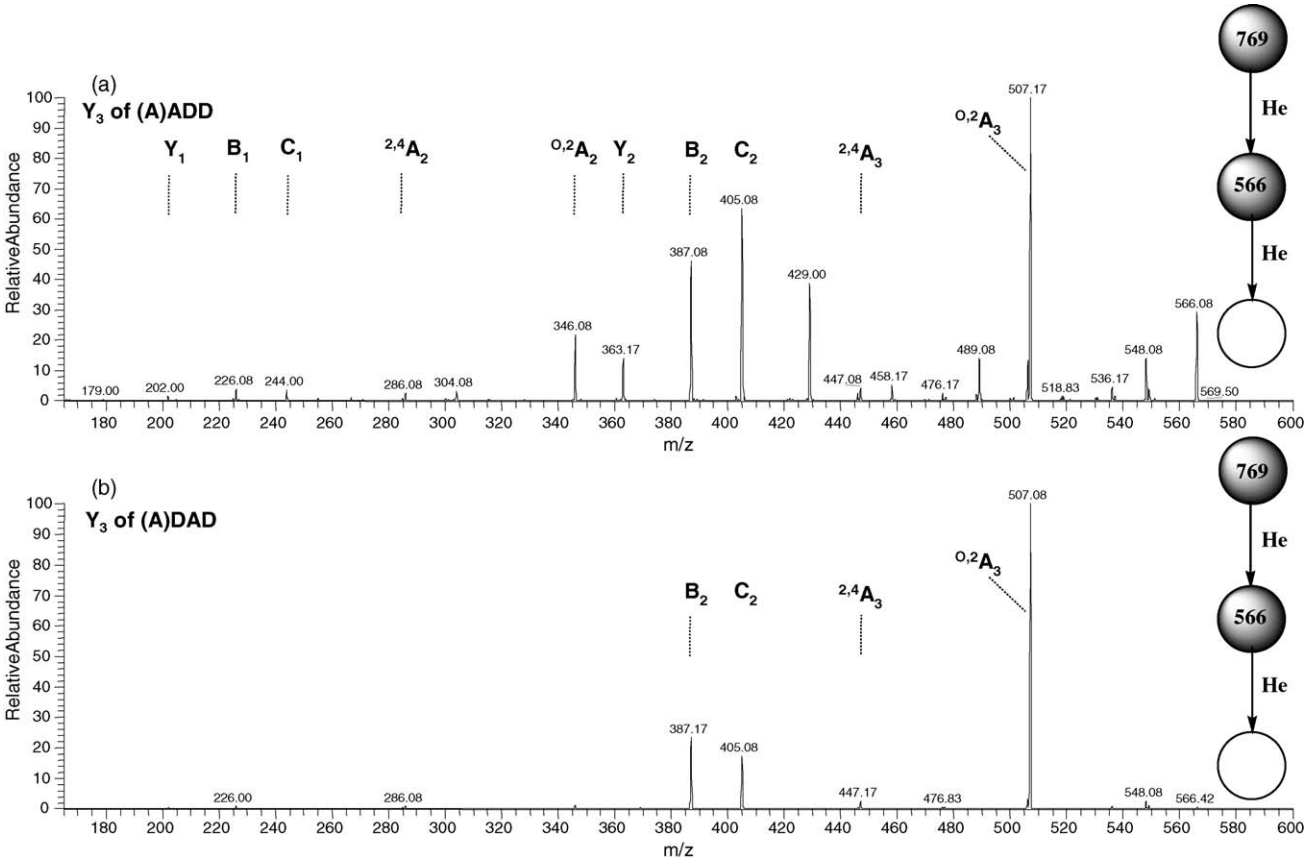

Fig. 11. MS^3 scan m/z 769 $[M+Na]^+ \rightarrow m/z$ 566 $[Y_3+Na]^+ \rightarrow$ products for (a) **AADD** (CE_{MS2} 15; CE_{MS3} 10), (b) **DADA** (CE_{MS2} 30; CE_{MS3} 12).

D heptasaccharide (Fig. S17). The base $[M-18+Na]^+$ ion of m/z 1276 and the $^{0,2}A_4$ $[M-101+Na]^+$ fragments of m/z 1193 are diagnostic for reducing end **A** isomers. The corresponding C_6/Y_6 and B_6 ions of m/z 1091 and 1073, respectively, are of the composition (**D_4A_2**). The MS^3 scan m/z 1294 → m/z 1091 → products shows the base $[C_6-18+Na]^+$ ion of m/z 1073 and cross-ring fragments of m/z 1032 $[C_6-59+Na]^+$ and 972 $[C_6-119+Na]^+$ of reducing-end **D**, as well as of m/z 990 $[C_6-101+Na]^+$ and 930 $[C_6-161+Na]^+$ of reducing end **A** residues, respectively (Fig. S18). According to rules 1 and 2, isomers **21**–**30**, containing **D** in the second position, are minor components. Otherwise, the MS^3 shows a series of rather low abundant C/Y- and B-type ions of m/z 930 and 912 (D_3A_2), 888 and 870 (D_4A), 769 (trace) and 751 (D_2A_2), 727 and 709 (D_3A), 608 (trace) and 590 (DA_2), 566 (trace) and 548 (D_2A), and 524 and 506 (trace) (D_3). In conclusion, none of the 15 isomers **21**–**35** can be excluded, though **31**–**35** having a reducing end partial sequence –**A**–**A** are obviously major components. Further analysis was not possible due to the low abundance of the fragment ions.

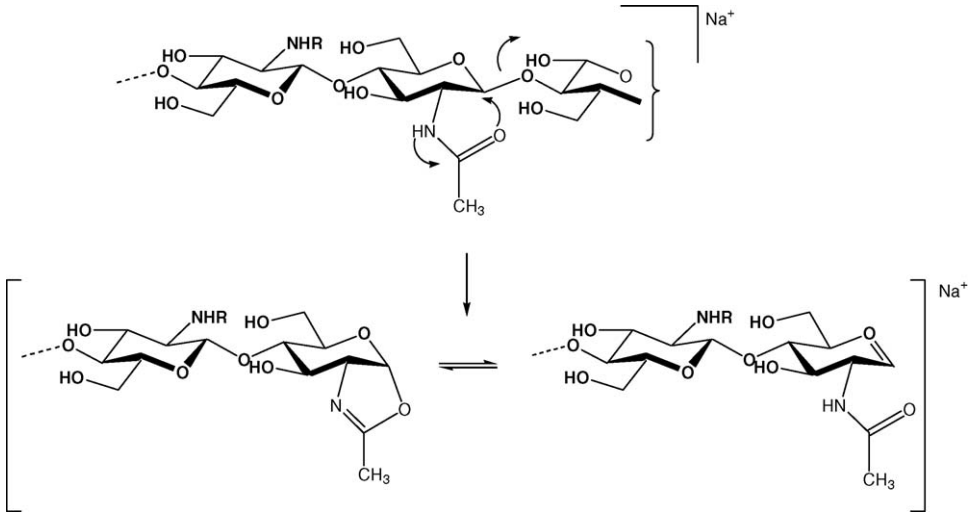

Fig. 12. Anchimeric assistance in B-type fragmentation of **A** residues.

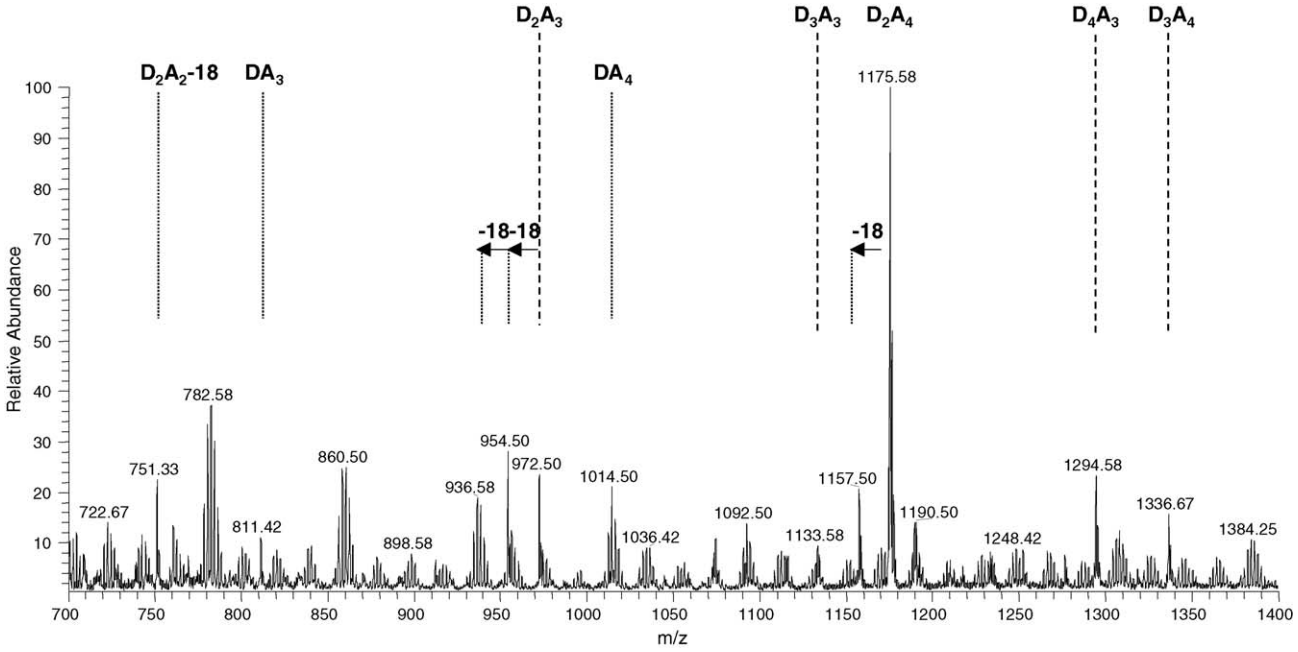

Fig. 13. ESI(+)-MS of a mixture of CHOs prepared by enzymatic degradation of chitosan.

3.13. MS^n of the $[M+Na]^+$ of m/z 1336 ($\mathbf{D_3A_4}$)

As for ($\mathbf{D_4A_3}$), 35 isomers are possible for the homologous heptasaccharide ($\mathbf{D_3A_4}$):

1. AAAADDD	**2**. AAADADD	**3**. AAADDAD	**4**. AADAADD	**5**. AADADAD
6. AADDAAD	**7**. ADAAADD	**8**. ADAADAD	**9**. ADADAAD	**10**. ADDAAAD
11. DAAAADD	**12**. DAAADAD	**13**. DAADAAD	**14**. DADAAAD	**15**. DDAAAAD
16. AAADDDA	**17**. ADDDAAA	**18**. DAAADDA	**19**. AADADDA	**20**. ADAADDA
21. DDDAAAA	**22**. DDADAAA	**23**. DADDAAA	**24**. DAADADA	**25**. DAADDAA
26. AADDDAA	**27**. AADDADA	**28**. ADADDAA	**29**. ADADADA	**30**. DDAADAA
31. DADADAA	**32**. ADDADAA	**33**. DDAAADA	**34**. DADAADA	**35**. ADDAADA

A $[M-59+Na]^+$fragment of *m/z* 1277 is absent in the MS^2 of the sodiated molecule of *m/z* 1336, thus excluding the 15 reducing-end **D** isomers (Fig. S19). The $[M-101+Na]^+$ ion of *m/z* 1235 is the $^{0,2}A_7$ cross-ring fragment of reducing end **A**. The $^{2,4}A_7$ $[M-161+Na]^+$ ion of *m/z* 1175 may contain also minor contributions from the isobaric Y_6, formed by loss of **D** from a non-reducing end. The C_6/Y_6 ion of *m/z* 1133 has the composition ($\mathbf{D_3A_3}$). The rather weak B_5 ion of *m/z* 912 ($\mathbf{D_3A_2}$) is consistent with isomers having a reducing end –**A**–**A** sequence. The corresponding B_5 ion of the composition ($\mathbf{D_2A_3}$), with calcd. *m/z* 954, is not detected. The MS^3 scan *m/z* 1336 $[M+Na]^+ \rightarrow$ *m/z* 1133 $\rightarrow$ products shows cross-ring fragments of both, reducing end **D** of *m/z* 1074 (weak) as well as **A** residues (Fig. S20). The appearance of two B_5 ions of *m/z* 954 ($\mathbf{D_2A_3}$) and 912 ($\mathbf{D_3A_2}$), but only one B_4 ion of *m/z* 751 ($\mathbf{D_2A_2}$), and only one

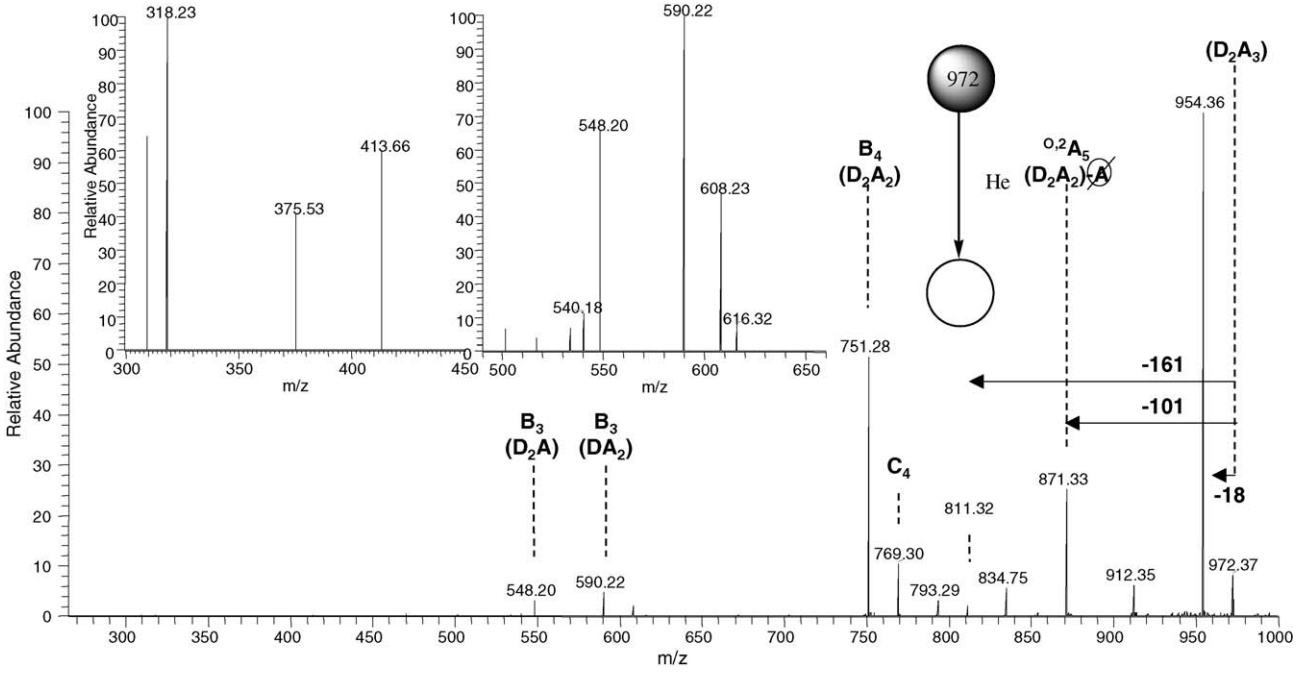

Fig. 14. MS^2 of the $[M+Na]^+$ ion of *m/z* 972 for ($\mathbf{D_2A_3}$) (CE 14.5). Inset: expansion in the *m/z* 300–450 and *m/z* 490–660 ranges, showing the absence of ions of *m/z* 650, 632 ($\mathbf{A_3}$), 363, and 345 ($\mathbf{D_2}$).

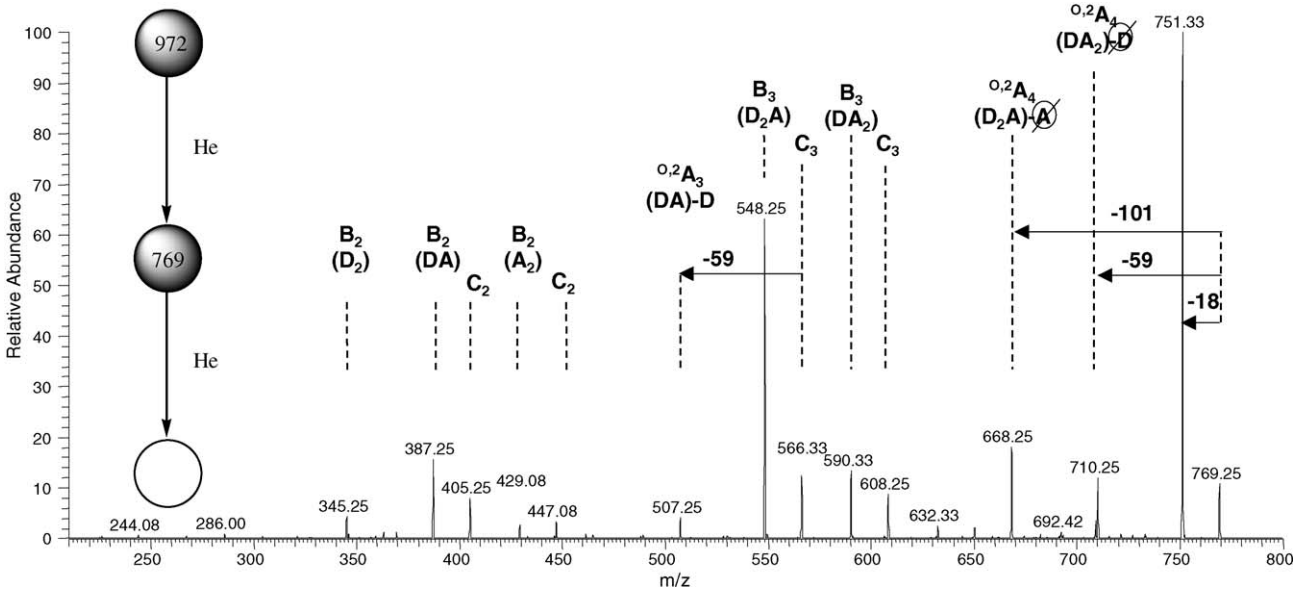

Fig. 15. MS^3 scan m/z 972 $[M+Na]^+ \rightarrow m/z$ 769 $[^{0,2}A_5+Na]^+ \rightarrow$ products for ($\mathbf{D_2A_2}$)-**A** (CE_{MS2} 13; CE_{MS3} 13).

B_3 ion of m/z 548 ($\mathbf{D_2A}$) excludes isomers **16** – **29**, because either B_4 or B_3 or both are mismatching, as Table 3 explains. For example, isomer **16** could give C_6 and Y_6 of the composition ($\mathbf{D_3A_3}$) which could fragment into two B_5 ($\mathbf{D_2A_3}$) and ($\mathbf{D_3A_2}$) and into B_4 ($\mathbf{D_2A_2}$) of Y_6 but not of C_6, and not into B_3 ($\mathbf{D_2A}$). Isomer **17** is excluded because C_6 must give B_4 ($\mathbf{D_3A}$) which is absent. All C_6 and some of the Y_6 ions of the six isomers **30**–**35** fragment into matching B_4 and B_3 ions. Those having a reducing end –**D**-**A** sequence, i.e. i.e. **33**–**35**, are minor components.

4. Conclusions

As described here for the six isomers of $\mathbf{D_2A_2}$ composition, collision induced dissociation via ESI(+)-MS^n (n = 2–4) of sodiated molecules of aminoglucan oligosaccharides $\mathbf{D}_m\mathbf{A}_n$ occurs via characteristic $^{0,2}A_n$ cross-ring and C/Y- as well as B-Type glycosidic bond cleavages. The reducing end sugar and its next neighbour is easily identified, allowing for the partial sequencing of components of mixtures of CHOs. Several isomers not present in a mixture can be reliably excluded, as shown with five examples of penta-, hexa-, and heptasaccharides where the prevailing reducing end sequence is –A–A. The results are similar to those published earlier for tagged hetero-CHOs (Bahrke et al., 2002; Haebel et al., 2007). As compared with conventional MS and NMR methods, the ESI(+)-MS^n method described herein has the advantage of being less invasive and time consuming since derivatizations, such as reducing end tagging and *N*-deuterioacetylation, are not required. The possibility of a sensitive, rapid, and direct ESI(+)-MS^n analysis of hetero-CHOs is particularly attractive for analysis of non-covalent protein–ligand complexes where any separation and chemical derivatization step would disturb the equilibrium between bound and free components. Applications of ESI(+)-MS^n are envisaged for the studies of the mechanisms of chitinolytic enzymes and the binding selectivity of chitolectins.

Table 3
Analysis of B-type ions generated in the ESI(+)-MS^3 scan m/z 1336 ($\mathbf{D_3A_4}$) → m/z 1133 ($\mathbf{D_3A_3}$) → products. Favoured fragmentation processes are indicated by (+) and disfavoured by (−).

m/z 1336 ($\mathbf{D_3A_4}$)	m/z 1133 $\mathbf{D_3A_3}$		m/z 751 $\mathbf{D_2A_2}$		m/z 548 $\mathbf{D_2A}$	
Isomer no.	C_6	Y_6	B_4 of C_6	B_4 of Y_6	B_3 of C_6	B_3 of Y_6
16. **AAADDDA**	**AAADDD** (−)	**AADDDA** (+)		**AADD** (−)		
17. **ADDDAAA**	**ADDDAA** (+)	**DDDAAA** (+)			**ADD**	
18. **DAAADDA**	**DAAADD** (−)			**DAA**		
19. **AADADDA**	**AADADD** (−)	**ADADDA** (+)		**ADAD** (−)	**AAD**	
20. **ADAADDA**	**ADAADD** (−)	**DAADDA** (+)		**DAAD** (−)		
21. **DDDAAAA**	**DDDAAA** (+)			**DDD**		
22. **DDADAAA**	**DDADAA** (+)			**DDA** (+)		
23. **DADDAAA**	**DADDAA** (+)			**DAD** (−)		
24. **DAADADA**	**DAADAD** (−)		**DAAD** (−)	**DAA**		
25. **DAADDAA**	**DAADDA** (+)		**DAAD** (−)	**DAA**		
26. **AADDDAA**	**AADDDA** (+)	**ADDDAA** (+)	**AADD** (−)		**AAD**	**ADD** (−)
27. **AADDADA**	**AADDAD** (−)	**ADDADA** (+)	**AADD** (−)	**ADDA** (+)	**AAD**	**ADD** (−)
28. **ADADDAA**	**ADADDA** (+)	**DADDAA** (+)	**ADAD** (−)		**ADA**	
29. **ADADADA**	**ADADAD** (−)	**DADADA** (+)	**ADAD** (−)	**DADA** (+)	**ADA**	**DAD** (−)
30. **DDAADAA**	**DDAADA** (+)		**DDAA** (+)	**DDA** (+)		
31. **DADADAA**	**DADADA** (+)		**DADA** (+)	**DAD** (−)		
32. **ADDADAA**	**ADDADA** (+)	**DDADAA** (+)	**ADDA** (+)		**ADD**	
33. **DDAAADA**	**DDAAAD** (−)		**DDAA** (+)	**DDA** (+)		
34. **DADAADA**	**DADAAD** (−)		**DADA** (+)	**DAD** (−)		
35. **ADDAADA**	**ADDAAD** (−)	**DDAADA** (+)	**ADDA** (+)	**DDAA** (+)	**ADD**	**DDA** (+)

Acknowledgements

This work was supported by Conselho Nacional de Desenvolvimento Científico e Tecnológico (CNPq), Coordenação de Aperfeiçoamento de Pessoal de Nível Superior (CAPES), and Fundação de Amparo à Pesquisa do Estado de São Paulo (FAPESP). MGP is especially grateful to FAPESP for a visiting research scholarship (08/01663-5).

Appendix A. Supplementary data

Supplementary data associated with this article can be found, in the online version, at doi:10.1016/j.carbpol.2010.04.041.

References

Bahrke, S. (2007). Mass spectrometric analysis of chitooligosaccharides and their interaction with proteins. PhD Thesis, University of Potsdam. URL: http://opus.kobv.de/ubp/volltexte/2008/2017/.

Bahrke, S., Einarsson, J. M., Gislason, J., Haebel, S., Letzel, M. C., Peter-Katalinić, J., et al. (2002). Sequence analysis of chitooligosaccharides by matrix-assisted laser desorption ionization postsource decay mass spectrometry. *Biomacromolecules*, *3*, 696–704.

Bakkers, J., Semino, C. E., Stroband, H., Kijne, J. W., Robbins, P. W., & Spaink, H. P. (1997). An important developmental role for oligosaccharides during early embryogenesis of cyprinid fish. *Proceedings of the National Academy of Sciences of the United States of America*, *94*, 7982–7986.

Bosso, C., & Domard, A. (1992). Characterization of glucosamine and *N*-acetylglucosamine oligomers by fast atom bombardment mass spectrometry. *Organic Mass Spectrometry*, *27*, 799–806.

Budnik, B. A., Haselmann, K. F., Elkin, Y. N., Gorbach, V. I., & Zubarev, R. A. (2003). Applications of electron-ion dissociation reactions for analysis of polycationic chitooligosaccharides in Fourier transform mass spectrometry. *Analytical Chemistry*, *75*, 5994–6001.

Budnik, B. A., Lee, R. S., & Steen, J. A. J. (2006). Global methods for protein glycosylation analysis by mass spectrometry. *Biochimica et Biophysica Acta*, *1764*, 1870–1880.

Cancilla, M. T., Wong, A. W., Voss, L. R., & Lebrilla, C. B. (1999). Fragmentation reactions in the mass spectrometry analysis of neutral oligosaccharides. *Analytical Chemistry*, *71*, 3206–3218.

Cederkvist, F., Zamfir, A. D., Bahrke, S., Eijsink, V. G. H., Sørlie, M., Peter-Katalinić, J., et al. (2006). Identification of a high-affinity-binding oligosaccharide by (+) nanoelectrospray quadrupole time-of-flight tandem mass spectrometry of a noncovalent enzyme-ligand complex. *Angewandte Chemie-International Edition*, *45*, 2429–2434.

Cederkvist, F. H., Parmer, M. P., Varum, K. M., Eijsink, V. G. H., & Sørlie, M. (2008). Inhibition of a family 18 chitinase by chitooligosaccharides. *Carbohydrate Polymers*, *74*, 41–49.

Domon, B., & Costello, C. E. (1988). A systematic nomenclature for carbohydrate fragmentations in FAB-MS/MS spectra of glycoconjugates. *Glycoconjugate Journal*, *5*, 397–409.

dos Santos, A. L. W., El Gueddari, N. E., Trombotto, S., & Moerschbacher, B. M. (2008). Partially acetylated chitosan oligo- and polymers induce an oxidative burst in suspension cultured cells of the Gymnosperm *Araucaria angustifolia*. *Biomacromolecules*, *9*, 3411–3415.

Einarsson, J. M., Gislason, J., Peter, M. & Bahrke, S. (2003). Pharmaceutical composition comprising chito-oligomers. WO 03/026677 (Primex Ehf., Iceland), 30 pp.

Fernandez, L. E. M. (2007). Introduction to ion trap mass spectrometry: Application to the structural characterization of plant oligosaccharides. *Carbohydrate Polymers*, *68*, 797–807.

Germer, A., Muegge, C., Peter, M. G., Rottmann, A., & Kleinpeter, E. (2003). Solution- and bound-state conformational study of *N*,*N*′,*N*″-triacetyl chitotriose and other analogous potential inhibitors of hevamine: Application of trNOESY and STD NMR spectroscopy. *Chemistry: A European Journal*, *9*, 1964–1973.

Haebel, S., Bahrke, S., & Peter, M. G. (2007). Quantitative sequencing of complex mixtures of heterochitooligosaccharides by vMALDI-linear ion trap mass spectrometry. *Analytical Chemistry*, *79*, 5557–5566.

Houston, D. R., Shiomi, K., Arai, N., Omura, S., Peter, M. G., Turberg, A., et al. (2002). High-resolution structures of a chitinase complexed with natural product cyclopentapeptide inhibitors: Mimicry of carbohydrate substrate. *Proceedings of the National Academy of Sciences of the United States of America*, *99*, 9127–9132.

Issaree, A. (2008). Synthesis of hetero-chitooligosaccharides. PhD Thesis, University of Potsdam. URL: http://opus.kobv.de/ubp/volltexte/2008/1706/.

Kim, S. K., & Rajapakse, N. (2005). Enzymatic production and biological activities of chitosan oligosaccharides (COS): A review. *Carbohydrate Polymers*, *62*, 357–368.

Mathesius, U. (2003). Conservation and divergence of signalling pathways between roots and soil microbes—The *Rhizobium*-legume symbiosis compared to the development of lateral roots, mycorrhizal interactions and nematode-induced galls. *Plant and Soil*, *255*, 105–119.

Peter, M. G. (2002a). Chitin and chitosan from fungi. In A. Steinbüchel (Ed.), *Biopolymers* (pp. 123–157). Weinheim: Wiley-VCH.

Peter, M. G. (2002b). Chitin and chitosan from animal sources. In A. Steinbüchel (Ed.), *Biopolymers* (pp. 481–574). Weinheim: Wiley-VCH.

Peter, M. G., & Eberlin, M. N. (in press). Applications of mass spectrometry to analysis of structure and bioactivity of chitooligosaccharides. In S.-K. Kim (Ed.), *Chitin, chitosan, oligosaccharides and their derivatives*. Boca Raton: CRC Press, pp. 127–148.

Price, N. P. J. (1999). Carbohydrate determinants of *Rhizobium*-legume symbioses. *Carbohydrate Research*, *317*, 1–9.

Semino, C. E., & Allende, M. L. (2000). Chitin oligosaccharides as candidate patterning agents in zebrafish embryogenesis. *International Journal of Developmental Biology*, *44*, 183–193.

Singh, S., Gallagher, R., Derrick, P. J., & Crout, D. H. G. (1995). Glycosidase-catalyzed oligosaccharide synthesis: Preparation of the *N*-acetylchito-oligosaccharides penta-*N*-acetylchitopentaose and hexa-*N*-acetylchitohexaose using the β-*N*-acetylhexosaminidase of *Aspergillus oryzae*. *Tetrahedron Asymmetry*, *6*, 2803–2810.

Spaink, H. P. (2000). Root nodulation and infection factors produced by rhizobial bacteria. *Annual Review of Microbiology*, *54*, 257–288.

Trombotto, S., Ladaviere, C., Delolme, F., & Domard, A. (2008). Chemical preparation and structural characterization of a homogeneous series of chitin/chitosan oligomers. *Biomacromolecules*, *9*, 1731–1738.

Vaaje-Kolstad, G., Houston, D. R., Rao, F. V., Peter, M. G., Synstad, B., van Aalten, D. M. F., et al. (2004). Structure of the D142N mutant of the family 18 chitinase ChiB from *Serratia marcescens* and its complex with allosamidin. *Biochimica et Biophysica Acta: Proteins and Proteomics*, *1696*, 103–111.

Vaaje-Kolstad, G., Vasella, A., Peter, M. G., Netter, C., Houston, D. R., Westereng, B., et al. (2004). Interactions of a family 18 chitinase with the designed inhibitor HM508 and its degradation product, chitobiono-δ-lactone. *Journal of Biological Chemistry*, *279*, 3612–3619.

van Aalten, D. M. F., Komander, D., Synstad, B., Gaseidnes, S., Peter, M. G., & Eijsink, V. G. H. (2001). Structural insights into the catalytic mechanism of a family 18 exo-chitinase. *Proceedings of the National Academy of Sciences of the United States of America*, *98*, 8979–8984.

Van der Drift, K. M. G. M., Olsthoorn, M. M. A., Brull, L. P., Blok-Tip, L., & Thomas-Oates, J. E. (1998). Mass spectrometric analysis of lipo-chitin oligosaccharides. Signal molecules mediating the host-specific legume-Rhizobium symbiosis. *Mass Spectrometry Reviews*, *17*, 75–95.

Vander, P., Vårum, K. M., Domard, A., El Gueddari, N. E., & Moerschbacher, B. M. (1998). Comparison of the ability of partially *N*-acetylated chitosans and chitooligosaccharides to elicit resistance reactions in wheat leaves. *Plant Physiology*, *118*, 1353–1359.

Vårum, K. M., Anthonsen, M. W., Grasdalen, H., & Smidsrød, O. (1991a). Determination of degree of N-acetylation and the distribution of *N*-acetyl groups in partially *N*-deacetylated chitins (chitosans) by high field NMR spectroscopy. *Carbohydrate Research*, *211*, 17–23.

Vårum, K. M., Anthonsen, M. W., Grasdalen, H., & Smidsrød, O. (1991b). ^{13}C NMR studies of the acetylation sequences in partially *N*-deacetylated chitins (chitosans). *Carbohydrate Research*, *217*, 19–27.

Vijayakrishnan, B. (2008). Solution and solid phase synthesis of *N*,*N*′-diacetyl chitotetraoses. PhD Thesis, University of Potsdam. URL: http://opus.kobv.de/ubp/volltexte/2008/1883/.

Wolff, J. J., Amster, I. J., Chi, L. L., & Linhardt, R. J. (2007). Electron detachment dissociation of glycosaminoglycan tetrasaccharides. *Journal of the American Society for Mass Spectrometry*, *18*, 234–244.

Zhang, S., Van Pelt, C. K., & Henion, J. D. (2003). Automated chip-based nanoelectrospray-mass spectrometry for rapid identification of proteins separated by two-dimensional gel electrophoresis. *Electrophoresis*, *24*, 3620–3632.